Journal of Medicinal Chemistry

Article

Small Molecule Inhibitors of Cyclophilin D to Protect Mitochondrial Function as a Potential Treatment for Acute Pancreatitis

Emma Shore, Muhammad Awais, Neil Kershaw, Robert Gibson, Sravan Pandalaneni, Dianne Latawiec, Li Wen, Muhammad Ahsan Javed, David Criddle, Neil Berry, Paul O'Neill, Lu-Yun Lian, and Robert Sutton

J. Med. Chem., **Just Accepted Manuscript** • DOI: 10.1021/acs.jmedchem.5b01801 • Publication Date (Web): 07 Mar 2016

Just Accepted

ACS Publications

Journal of Medicinal Chemistry is published by the American Chemical Society. 1155 Sixteenth Street N.W., Washington, DC 20036

Small Molecule Inhibitors of Cyclophilin D to Protect Mitochondrial Function as a Potential Treatment for Acute Pancreatitis

Emma R. Shore[1], Muhammad Awais[2], Neil M. Kershaw[1], Robert R. Gibson[3], Sravan Pandalaneni[3], Diane Latawiec[2], Li Wen[2], Muhammad A. Javed[2], David N. Criddle[2], Neil Berry[1], Paul M. O'Neill[1*], Lu-Yun Lian[3*] and Robert Sutton[2]

[1] Department of Chemistry, University of Liverpool, Crown Street, Liverpool L69 7ZD, [2]NIHR Liverpool Pancreas Biomedical Research Unit, Institute of Translational Medicine, University of Liverpool, Royal Liverpool University Hospital, Daulby Street, Liverpool L7 8XP and [3] Institute of Integrative Biology, Biosciences Building, University of Liverpool, Crown Street, Liverpool L69 7ZD, United Kingdom

ABSTRACT

Opening of the mitochondrial permeability transition pore (MPTP) causes mitochondrial dysfunction and necrosis in acute pancreatitis (AP), a condition without specific drug treatment. Cyclophilin D (CypD) is a mitochondrial matrix peptidyl-prolyl isomerase that regulates the MPTP and is a drug target for AP. We have synthesised urea-based small molecule inhibitors of cyclophilins and tested them against CypD using binding and isomerase activity assays. Thermodynamic profiles of the CypD/inhibitor interactions were determined by isothermal titration calorimetry. Seven new high-resolution crystal structures of CypD-inhibitor complexes were obtained to guide compound optimisation. Compounds **4**, **13**, **14** and **19** were tested in freshly isolated murine pancreatic acinar cells (PACs) to determine inhibition of toxin-induced loss of mitochondrial membrane potential ($\Delta\Psi_m$) and necrotic cell death pathway activation. Compound **19** was found to have a K_d of 410 nM and favourable thermodynamic profile, showed significant protection of $\Delta\Psi_m$ and reduced necrosis of murine as well as human PACs. Compound **19** holds significant promise for future lead optimisation.

INTRODUCTION

Acute pancreatitis (AP) is a common pancreatic disease predominantly caused by gallstones or excessive alcohol intake. Pancreatic necrosis, systemic inflammatory response syndrome, multiple organ failure and sepsis are characteristic of severe AP, which results in the death of one in four patients.[1, 2] Despite approximately 300 randomised clinical trials in human AP and about 700 publications evaluating agents in preclinical studies, there is still no internationally validated specific drug therapy for human AP.[3]

Mitochondrial dysfunction is central to the pathogenesis of AP as well as other diseases including ischemia-reperfusion injury of the heart, brain and kidney, muscular dystrophies and neuro-degeneration.[4-10] Mitochondrial dysfunction is the result of a sudden increase in permeability of the inner mitochondrial membrane (IMM), via persistent opening of a multi-protein channel known as the mitochondrial permeability transition pore (MPTP).[6] This allows uncontrolled proton flow across the IMM and unregulated flux of water, ions and solutes up to 1.5 kDa into and out of the mitochondrial matrix. A resultant loss of mitochondrial membrane potential ($\Delta\Psi_m$) essential for ATP production, coupled with disruption of calcium homeostasis, activates the necrotic cell death pathway.[6, 11, 12]

In 1984 Fischer *et al*. found a protein that accelerated efficiently the *cis-trans* isomerization of prolyl peptide bonds in short oligopeptides.[13] This protein was named peptidyl-prolyl cis-trans isomerase (PPIase) which catalyses a 180 degree rotation about the C-N linkage of the peptide bond preceding proline.[14] Later, this was shown to be the protein called cyclophilin which binds very strongly to Cyclosporine A (CsA) (Figure 1).[15]

Cyclophilin D (CypD)[16] is the mitochondrial matrix protein with PPIase activity. It is best recognised as an important regulator of the MPTP.[16-18] We recently reported that MPTP opening is critical to multiple forms of AP, causing diminished ATP production, defective autophagy, zymogen activation, cytokine release and necrosis.[4] Pharmacological or genetic MPTP inhibition in murine or human PACs preserved $\Delta\Psi_m$, ATP production, autophagy and prevented necrosis in response to pancreatitis toxin-induced calcium release via inositol trisphosphate receptor (IP_3R) and ryanodine receptor (RyR) calcium channels.[4] This mechanism was confirmed in four *in vivo* models of AP. Thus, characteristic local and systemic pathological responses were greatly reduced or abolished in CypD knockout mice and in wild type mice treated with MPTP inhibitors, confirming that mitochondrial dysfunction through MPTP opening is a fundamental pathological mechanism in AP, which can be ameliorated by inhibition of CypD.[4, 16]

Cyclosporin A (CsA), a lipophilic cyclic peptide (Figure 1), has nanomolar binding affinity for cyclophilins (Cyps), most notably CypA, CypB and CypD.[19, 20] CsA is an immunosuppressant and is widely used as an anti-rejection drug in solid organ transplantation. The interaction of CsA with cytosolic CypA generates a complex that has an ability to bind to, and inhibit calcineurin. As a consequence, the calcineurin substrate, phospho-nuclear factor of activated T-cells (pNFAT), is unable to translocate to the nucleus and initiate an immune response.[21] Non-immunosuppressant semi-synthetic analogues of CsA such as Debio 025 and NIM811 (Figure 1) maintain inhibition of Cyps but do not bind to calcineurin.[20] However, these inhibitors have unfavourable drug-like characteristics with high molecular weights, limited solubility and poor bioavailability.[22] Small molecule

inhibitors are needed that exhibit high selectivity for CypD over other Cyps, have improved pharmacokinetic/pharmacodynamic (PK/PD) properties and do not exhibit immunosuppression, to treat acute pancreatitis and other diseases in which mitochondrial dysfunction has a major role.

A number of compounds have previously been identified as potent inhibitors of Cyps, several with nanomolar activities.[23-26] We synthesised and tested compounds **1-4** shown in Figure 2. In our hands, the poorly soluble analogues **1-3** gave variable results in both PPIase and calcium retention capacity (data not shown) assays making them unsuitable for further optimisation. On the other hand, compound **4** gave consistent results when tested for PPIase inhibition in the presence and absence of the detergent NP40. These preliminary data accord with those of Colliandre *et al.*, who have disclosed a range of Cyp inhibitors based on a urea template in two separate patents.[24, 25] They identified compound **4** to exhibit moderate binding selectivity for CypB and CypD over CypA with an IC_{50} of 6.1, 6.2 and 16.8 μM, respectively. The authors also determined the X-ray structure of compound **4** in complex with CypD (PDB: 3RDC).

CypD has two adjacent binding pockets (S1' and S2, Figure 3a), both of which might be exploited. Based on the crystal structures of CypA and peptides/proteins (PDB: 1FGL, 1AK4, 1AWR), the S1' site is where the proline binds (Figure 3b). Residues around the S2 pocket interact with peptide residues -2 and -3 relative to the native proline substrate. In the complexes of CsA with CypA and D (PDB: 1IKF, 2Z6W), Mva (*N*-methyl-*L*-valine) occupies the S1' pocket and superimposes well with the proline residue of the peptide ligand. Aba (*L*-α-aminobutyric acid) is located in the S2 site and the Bmt ((4*R*)-4[(E)-2-butenyl]-4,N-dimethyl-*L*-threonine) binding defines

the S1 site (Figure 3c). Compound **4** binds in the S2 and S1' binding pockets (PDB: 3RDC), and is schematically depicted in Figure 3d.

Here we report the development of urea-based inhibitors of CypD starting from compound **4**. We aimed to identify an optimal template for the S2 and S1' sites by first addressing S2 to allow for further development in a rational manner. The interactions between the synthesised compounds and sites S2 and S1' of CypD were systematically characterised using X-ray crystallography to obtain high-resolution structures of the complexes and isothermal titration calorimetry (ITC) to derive the thermodynamic signature of the interactions. PPIase assays were performed for selected compounds and the most promising analogues were tested in freshly isolated murine and human PACs for their ability to inhibit pancreatitis toxin-induced loss of $\Delta\Psi_m$ and necrotic cell death pathway activation. Through the synthesis of enantiomerically pure compounds, we were able to resolve which enantiomer affords optimal potency. The outcome of these studies demonstrated that the enthalpy-entropy compensation poses a challenge in the rational structure-based design of potent inhibitors, even though high-resolution X-ray crystal structures of the complexes were available at each stage of the design process.

RESULTS AND DISCUSSION

In-vitro inhibition studies of compounds 1-4. Compounds **1** and **2** were identified and reported by Ni *et al.* to have IC_{50} values of 1.52 nM and 159 nM, respectively, in a chymotrypsin-coupled PPIase assay with CypA.[23] Notably, **1** was highlighted as being a more potent CypA inhibitor than CsA. Guichou *et al.* described a range of diarylureas as CypA inhibitors, identifying **3** to be the most promising lead with an IC_{50} of 14 nM in a chymotrypsin-coupled PPIase assay.[26] Compound **4**, a

urea based template, was identified by Colliandre *et al.* Although the activity was modest in comparison with those reported for compounds **1**-**3**, some desirable selectivity for CypD over CypA was reported.[24, 25] The same group deposited an X-ray crystal structure of **4** in the active site of CypD (PDB: 3RDC), enabling structure-based drug design approaches to be adopted.

We performed PPIase assays against CypD with compounds **1-4** in the absence and presence of a detergent to identify non-specific inhibitors. Disappointingly, **1**-**3** did not exhibit any reproducible activity against CypD, most likely due to promiscuous behaviour as their interaction with the protein involved aggregation of the compounds.[27, 28] Additionally, extremely low solubilities precluded the use of ITC and X-ray crystallography for further analyses. However, **4** had a K_i of 2.9 μM without detergent, which was only slightly perturbed upon addition of detergent. Furthermore using ITC, **4** bound to CypD with a K_d of 10.0 μM, consolidating the result observed in the PPIase assay. On the basis of these results, **4** was taken forward for further investigations.

Molecular docking of compound 4 and analogues. An undesirable feature of **4** is the aniline functional group that is a known metabolic alert;[29] hence, the chemical space around the aniline was probed to determine other substituents that might be tolerated. Additionally, as the ester is a metabolically labile functional group, amide replacements were investigated to improve chemical and metabolic stability.[30] Molecular modelling was used to predict both the mode and strength of compound binding. A docking protocol was developed that reproduced the binding pose of **4** with CypD (RMSD, 0.53Å) accurately. Once validated, this protocol was

employed to dock the compounds in Table 1. All compounds bound in a very similar fashion to **4**. The ChemPLP binding scores were very similar to **4** (see Supporting Information S1), providing confidence in the synthesis of a library of compounds, representative examples of which are shown in Table 1. ITC, PPIase inhibition and X-ray crystallographic studies were undertaken for these compounds.

Chemical synthesis of compound 4 analogues. Compounds **5**-**9** were synthesised by reaction of the appropriate amine with ethyl isocyanatoacetate (Scheme 1A). An alternative strategy was employed for the synthesis of **10**-**19** wherein 4-aminobenzylamine was first converted to the corresponding CDI-adduct. This was then coupled to a variety of amino esters and amides to afford the requisite ureas (Scheme 1B). Table 1 summarises the chemical structures of these compounds.

Guided by the Colliandre patent, which demonstrates high potency for 2-aryl pyrrolidine analogues, we sought to define the absolute stereochemical requirements for good inhibition of CypD as well as to determine the thermodynamic characteristics and binding pose.[24, 25] The chiral *ortho*-substituted-2-arylpyrrolidine motif present in **12**, **13**, **18** and **19** represented a significant synthetic challenge. Whilst the synthesis of chiral 2-arylpyrrolidines via asymmetric hydrogenation of cyclic enamines is well established, *ortho*-substituents on the aromatic ring are poorly tolerated.[31, 32] Instead, a strategy relying on asymmetric reduction of an acyclic precursor was devised and is shown in Scheme 2. Addition of the appropriate Grignard reagent to commercially available *N*-Boc-2-pyrrolidinone afforded the protected amino ketone **20**. Enantioselective reduction using the CBS-

oxazaborolidine reagent established the necessary stereocentre in **21** with good enantiomeric ratios. Conversion of the alcohol to the mesylate gave **22,** amine deprotection and cyclisation gave the desired 2-arylpyrrolidines **23a** and **23b** in excellent yield. **23c** was synthesised in an analogous fashion using the enantiomeric CBS-oxazaborolidine reagent. **23** was then coupled to Boc-Gly-OH or Boc-Met-OH to yield **24** and **25,** respectively.

Isothermal titration calorimetry (ITC). Figure 4 shows a subset (compounds **4**, **10, 12, 14, 11** and **19)** of ITC profiles for the binding of synthesised compounds. The experimental data were analysed using a single-site binding model and in all cases the compounds bound with a stoichiometry of 1:1, as is also observed in the respective crystal structures.

(i) Compounds 4-9 (S2 site). Of all the compounds tested to probe the S2 site, compound **4** displayed the best affinity**.** Modifications of the aniline portion of the molecule indicated that this portion of the binding site is highly sensitive to modification. The data summarised in Table 1 and Figure 5a show **4** binding in an enthalpically-driven manner with ΔG ~ -6.8 kcal/mol, a ΔH ~ -13.7 kcal/mol and $-T\Delta S$ ~ 6.9 kcal/mol, similar to CsA. In the CypD-**4** crystal complex, a water molecule forms a network of hydrogen bonds involving the amine group of the aniline moiety and residues A101, G109 and Q111, whereas with **5**-**9** these hydrogen bonds are not formed. Work is currently in progress to more fully explore the structure-activity relationships of this site.

(ii) Compounds 10-13 (S1' site). The thermodynamic parameters for **10-13** are shown in Figure 5b. The pyrrolidine in **10** sits in the active site (PDB 4J58) at the

same position as the proline residue in the 'natural' substrate. The significant improvement in entropic contributions to binding of **10** over **4** is negated by a compensatory loss of enthalpy.[33] In **4**, a hydrogen bond is formed between the ether oxygen of the ethyl ester and Arg55. The absence of this oxygen in **10** results in the loss of this hydrogen bond, hence, a much smaller observed ΔH value. Addition of a phenyl group to the 2-position of the pyrrolidine ring, compound **11**, resulted in an improved K_d of 5.4 μM.

The C-2-aryl analogues reported by Colliandre *et al.* had undefined stereochemistry in the majority of cases.[24, 25] We established that the *R*-stereoisomer is the preferred form for binding to CypD. Compound **12** binds with a higher affinity than **10,** obtained through an enthalpy gain due to an extra hydrogen bond between Arg55 and the carbonyl oxygen of the urea backbone (PDB 4J5B). Compound **13** is analogous to **12** with the *ortho*-thiomethyl replaced by an *ortho*-bromo and binds with a K_d of 1.2 μM. The results for **11-13** suggest that the phenyl group on the pyrrolidine ring markedly affects how the compound binds in the S1' site, in addition to the *ortho*-substituent playing an important role in binding.

(iii) Compounds 14-17 (S1 site). Substitutions at the R- position (Scheme 1 and Table 1) aim to probe the possibility of mimicking the Bmt group of CsA (Figure 3). In the CypD-CsA complex, (PDB: 2Z6W) the Aba2-Bmt1-Mva11 group makes a primary hydrophobic and hydrogen bond interaction along the Cyp active site groove.[34] The data in Table 1 shows that the (*S*)-methionine side chain in **14** confers the best affinity and was therefore retained in the final compound investigated, compound **19**.

(iv) Compound 19. Colliandre *et al.* reported their best compound to have an IC_{50} of 0.66 μM against CypD and this molecule is presumed to be a racemic mixture of 4 diastereoisomers.[25] Here, an asymmetric synthesis of their lead compound was undertaken to give 2 diastereoisomers; compounds **18** and **19**. Compound **19** has a K_d of 0.41 μM and a K_i of 99 nM whereas the K_d for **18** is 82 μM making *R* the stereochemistry required for the aryl group on the pyrrolidine. Compound **19** (Figure 5c) compared to **4** shows a significant entropy gain that is larger than the enthalpy loss, resulting in ΔG (**19**) of -8.7 kcal/mol and ΔG (**4)** of -6.8 kcal/mol. The entropic gain is due to an increase in hydrophobic interactions between hydrophobic residues lining the S1' site (Ile57, Ile60, Met61, Phe102 and Leu122) and the *o*-thiomethyl phenyl group. There is an enthalpy loss on binding of **19** to CypD compared to **4**. Nevertheless the crystal structure showed that the important hydrogen bonds are preserved between the CypD-complex of **4** and **19**, therefore this enthalpy loss must be due to another factor (*vide infra)*.

The marked enthalpy-entropy compensation effect observed for the series of compounds described is not uncommon for many biomolecular interactions,[35] particularly in the binding of structurally similar ligands and when interactions are weak. The enthalpy-entropy compensation here is most likely attributed to the inherent conformational flexibility and dynamics of the protein structure, as observed for the analogous protein, CypA.[36, 37] In addition a reorganisation of water molecules occurs in some cases (*vide infra)*.

X-ray crystallography. In this study, the crystal structures (PDB: 5CBT, 5CBU, 5CBV, 5CCN, 5CBW, 5CCS, 5CCR) were determined to resolutions of 1.4-2.1Å. Apart from some variations in the unstructured regions Asp66-Gly74 and Ser144-Ile156, the most notable feature observed from the various structures is how the orientations of Arg82 and Arg55 side-chains affect the topology of the binding site.

In either the free protein or the aniline compound complexes (Table 1), the Arg82 side-chain forms one side of the S2 pocket, creating a more compact pocket (Figure 6a). When other groups replace the aniline moiety (compounds **5-9**), Arg82 consistently moves away, leading to a more open S2 pocket (Figure 6b and 6c). Although the aniline group provides capacity for hydrogen bonding, this alone is not sufficient to determine the orientation of the Arg82 side-chain; complexes with **10, 12, 13** and **14** show Arg82 adopting both the 'open' and 'closed' conformations. Thus 'R' and 'X' substitutions (Table 1) appear to have subtle effects that alter the orientation of the Arg82 side-chain. The flexibility of Arg82 appears to enable the protein to bind to larger compounds; interestingly, Arg82 adopts the open conformation in the CypD-CsA complex (PDB 2Z6W). This suggests that Arg82 may have a role in interactions with specific protein partners since this residue is not conserved across CypA, CypB, CypC or CypE in what is an otherwise highly conserved binding site.[38]

The S1' binding pocket also exhibits structural variation, centred on Arg55. The binding conformation of the ester in **4-9** is conserved, primarily with hydrogen bonds between Arg55-Nω and the ether oxygen atom of the ethyl ester. The interaction is reinforced though a hydrogen bonding network between Arg55 and Gln63

throughout this initial set of structures (Figure 6d). In the complex with **10** the absence of the Arg55-Nω to ester oxygen inter-molecular hydrogen bond results in a 41.3° rotation of the guanidinium moiety out of the pocket, and subsequent hydrogen bonding to two water molecules. This is further exemplified by **11, 12, 13, 18** and **19** where steric hindrance from the aromatic ring substituents force the Arg55 side-chain outwards (Figure 6d), forming a hydrogen bond with the urea carbonyl and causing a 24.4° puckering to the substituted pyrrole ring with respect to the unsubstituted pyrrole ring of **10**.

The most promising compound, **19**, is bound to the active site of CypD through a large number of cooperative non-covalent interactions (Figure 7). The amino group forms a hydrogen bond network (coloured red) via co-crystallised water molecules to the protein, involving residues Thr107 to Gln111. Aromatic π-π stacking interactions (orange) are observed between the aniline ring and Asn102 and Gln111. The central urea motif forms multiple hydrogen bonding contacts that include hydrogen bond donation and hydrogen bond donor-π interactions (yellow) with Asn102 (red) whilst the carbonyl functionality forms bonding interactions via a crystallised water molecule with His54, Gly72 and Arg55 (the interaction with the latter is a cation-dipole interaction). The enhanced strength of the binding of **19** may be attributed to the large number of van der Waals interactions that are made between the ortho-substituted pyrrolidine with Arg55, Ile57, Phe60, Phe113, Leu122 and His126 and also an edge to face π-π interaction of the thiomethyl substituted ring with Phe60. The conformation of Arg55 is different for **19** compared with compound **4** due to the large thiomethyl ortho substitution on the benzene ring. With **19 t**he Arg55 is involved in hydrogen bonding with the carbonyl group of the urea and also a cation-

dipole interaction with a crystallographic water – both of these interactions are not observed in initial compound **4**.

Cellular assays using freshly isolated PACs. Informed by the *in vitro* data obtained for the series, we selected **4**, **13**, **14** and **19** to obtain proof of principle studies in freshly isolated PACs, the initial site of injury in AP.[39] We evaluated the ability of the CypD inhibitors **4**, **13**, **14** and **19** to inhibit necrotic cell death pathway activation in freshly isolated murine PACs in the presence of a pancreatitis toxin, taurolithocholate acid 3-sulphate (TLCS, 500 μM), and compared the effect of the inhibitors with CsA in a concentration dependent manner. TLCS depolarises mitochondria and induces necrosis in PACs from loss of ATP production. [4, 40-42] Parallel experiments were conducted in which PACs were exposed to CsA, **4, 13, 14** and **19** without TLCS, to determine primary cytotoxic effects of these compounds. As shown in Figure 8a, CsA and 19 were tested at 0.1, 1.0 and 10 μM while **4**, **13** and **14** were tested at 1 and 10 μM. CsA provided significant protection with each concentration used. Compound 4 did not reduce necrosis significantly at 1.0 and 10 μM; compounds **13** and **14** provided significant protection at 10 μM but not 1 μM. Compound **19** provided significant protection from necrotic cell death pathway activation at both 1 and 10 μM, likely due to its high binding affinity and strong inhibitory effect on CypD enzymatic activity (Table 1) (although some of the necrosis inhibition and membrane potential protection do not directly correlate with the *in-vitro* affinity assays and this could be due to differences in the stability and/or cell permeability). None of the compounds except **13** (10 μM) showed significant primary cytotoxicity in this assay (S5). To confirm that the reduction of necrosis in PACs resulted from the maintenance of mitochondrial function by preventing the opening of

the MPTP, we performed $\Delta\Psi_m$ assays in freshly isolated PACs loaded with the positively charged mitochondrial dye tetramethyl rhodamine methyl ester (TMRM). Figure 8b shows a decrease in $\Delta\Psi_m$ in response to TLCS that was ameliorated in the presence of **13**, **14** and **19**, indicating protection of $\Delta\Psi_m$. The potential applicability of **19** as a treatment for human AP is demonstrated by its effects in freshly isolated human PACs (obtained from fully informed and consenting patients undergoing pancreatic resectional surgery). As shown in Figure 8c, **19** at 10 μM prevented necrotic cell death pathway activation in human PACs.

CONCLUSION

We have designed, optimized and synthesized a series of analogues and enantiomers (**5-19**) of the hit compound **4** to develop competitive inhibitors of CypD with potential protective activity against cellular necrosis. Compound **19** shows enzymatic inhibition in the nanomolar range. Thermodynamic profiling of each interaction together with the high-resolution crystal structures of each complex was integral in optimisation. The structures show the important roles played by the local flexibility within the CypD structure, reflected in variations in the orientations of side-chains Arg55 and Arg82, both of which form direct and indirect hydrogen bonds via water molecules with the different compounds. Cellular assays using freshly isolated murine and human PACs showed that cells treated with the highest affinity compound **19** were capable of inhibiting both loss of $\Delta\Psi_m$ and activation of the necrotic cell death pathway induced by a bile acid. We provide here one of the few examples of a drug development project where thermodynamic profiling coupled to molecular modelling and structure determination has been systematically used to

provide improvements in the efficacy of the compounds. The urea compound **19** could, therefore, serve as a lead compound for further development of small molecule agents against AP.

EXPERIMENTAL SECTION

Chemistry General Information:

All reactions were carried out employing standard chemical techniques under an inert atmosphere. Solvents used for extraction, washing, and chromatography were HPLC grade. Chemicals were purchased from Sigma Aldrich, Fluorochem or Apollo and used without further purification. Purity values for all tested compounds were found to be above 95% from either combustion analysis (**4-7**, **9**-**11** and **14**-**16**) or high-performance liquid chromatography (HPLC) analyses on an Agilent 1200 (**8**, **12**-**13** and **17**-**19**). Absolute stereochemistry was determined by analytical HPLC using a chiral stationary phase. The column utilised was a CHIRALPAK AD-H column using a flow rate of 1.2ml/min eluting with 15% IPA in hexane. Retention times, t_R, of the products are reported in minutes and (%) purity at 210 or 254 nm. Mass spectra were recorded on an Agilent QTOF 7200 mass spectrometer. When EI mass analysis was utilised, formic acid and methanol were used as the solvent systems. When CI mass analysis was utilised, ammonia was used as the carrier gas. All mass spectrometry and elemental microanalysis was done within the University of Liverpool's chemistry department. NMR spectra were recorded using a Bruker MX 400 MHz spectrometer. Chemical shifts are listed as δ values in ppm downfield from an internal standard of tetramethylsilane. Infrared spectra were recorded using a PerkinElmer1720-x FT-IR spectrometer. Melting points were recorded manually using a Gallenkamp melting point apparatus.

Chemistry General Procedures:

General procedure A (4-9) – Ethyl isocyanatoacetate (1 eq) was dissolved in DMF (0.14 M). The given amine (1 eq) was added and the reaction mixture was stirred at room temperature for 2 hours. After this time, the solvent was removed *in vacuo* to yield the crude product.

General procedure B (10-13 and **17-19)** – The given Boc-protected amino amide derivative (1eq) was first dissolved in a mixture of dichloromethane and trifluoroacetic acid, 5:1 (0.1 M) and stirred for 1 hour then concentrated *in vacuo* to afford the corresponding amino amide as a trifluoroacetate salt which was used without further purification. 4-aminobenzylamine (1 eq) was dissolved in DCM (0.1M) and the reaction mixture was cooled to 0°C. CDI (1.1 eq) and DMAP (0.1 eq) were added and the reaction mixture was stirred at r.t overnight. After this time, the reaction mixture was diluted with EtOAc and washed with water. The organic layer was dried over $MgSO_4$, filtered and concentrated *in vacuo* to yield a yellow solid that required no further purification. Both the amino amide as the trifluoroacetate salt (1 eq) and the CDI adduct (1 eq) were dissolved in acetonitrile (0.1 M) and triethylamine (2.2 eq) was added. The resulting suspension was stirred at room temperature for 16 hours. After this time, the solvent was removed *in vacuo* to yield the crude product.

General Procedure C (14-16) – The given amino acid ethyl ester as its hydrochloride salt (1 eq) was dissolved in acetonitrile (0.1 M) and triethylamine (2.2 eq) was added followed by *N*-(4-aminobenzyl)-1*H*-imidazole-1-carboxamide (1 eq) in a single portion. The resulting suspension was stirred at room temperature for 16 hours. After this time, the solvent was removed *in vacuo* to yield the crude product.

Ethyl 2-(3-(4-aminobenzyl)ureido)acetate (4). The crude product was triturated with diethyl ether to yield a white solid (156 mg, 0.62 mmol, 8%). M.p: 164 – 166°C; IR v_{max} (cm^{-1}) 1207 (C-O), 1564 (N-H), 1610 (amide C=O), 1732 (ester C=O), 3348 (N-H); ^{1}H NMR (400MHz; $CDCl_3$; Me_4Si; ppm) δ 7.09 (2H, ap: d, *J* = 8.4), 6.65 (2H, ap: d, *J* = 8.4), 4.87 (1H, t, *J* = 5.4), 4.74 (1H, t, *J* = 5.4), 4.25 (2H, d, *J* = 5.4), 4.18 (2H, q, *J* = 7.1), 3.99 (2H, d, *J* = 5.4), 3.65 (2H, s), 1.27 (3H, t, *J* = 7.1); ^{13}C NMR (100 MHz; $CDCl_3$; Me_4Si) δ 171.6, 158.0, 151.8, 129.3, 129.0, 115.6, 61.8, 44.8, 42.7, 14.6; HRMS (ES+) *m/z* 274.1159 $[M+Na]^+$ $C_{12}H_{17}N_3O_3Na$ requires 274.1168 (Diff -3.1 ppm). Anal. Calcd. for $C_{12}H_{17}N_3O_3$: C, 57.36; H, 6.82; N, 16.72. Found C, 57.28; H, 6.89; N, 16.81.

Ethyl 2-(3-benzylureido)acetate (5). The crude product was triturated with diethyl ether to yield a white solid (2.18 g, 9.23 mmol, 99%). M.p: 78 – 80°C; IR v_{max} (cm^{-1}) 1200 (C-O), 1574 (N-H), 1622 (amide C=O), 1745 (ester C=O), 3330 (N-H); ^{1}H NMR (400MHz; $CDCl_3$; Me_4Si; ppm) δ 7.32 – 7.22 (5H, m), 5.12 (2H, br s), 4.34 (2H, s), 4.13 (2H, q, *J* = 7.2), 3.95 (2H, s), 1.24 (3H, t, *J* = 7.2); ^{13}C NMR (100 MHz; $CDCl_3$; Me_4Si) δ 171.83, 158.45, 139.39, 129.01, 127.82, 127.69, 61.78, 44.86, 42.66, 14.51; HRMS (ES+) *m/z* 259.1057 $[M+Na]^+$ $C_{12}H_{16}N_2O_3Na$ requires 259.1059 (Diff -0.6 ppm); Anal. Calcd. for $C_{12}H_{16}N_2O_3$: C, 61.00; H, 6.83; N, 11.86. Found C, 59.66; H, 6.87; N, 12.04.

Ethyl 2-(3-(4-(pyridin-4-yl)benzyl)ureido)acetate (6). The crude product was triturated with diethyl ether to yield a white solid (72 mg, 0.23 mmol, 43%). M.p: 156 – 157°C; IR v_{max} (cm^{-1}) 1215 (C-O), 1574 (N-H), 1628 (amide C=O), 1732 (ester C=O), 3305 (N-H), 3386 (N-H); ^{1}H NMR (400MHz; $CDCl_3$; Me_4Si; ppm) δ 8.64 (2H, d, *J* = 5.3), 7.57 (2H, d, *J* = 8.1), 7.49 (2H, d, *J* = 5.5), 7.41 (2H, d, *J* = 8.1), 5.31 (1H, t, *J* = 5.6), 5.27 (1H, t, *J* = 5.2), 4.45 (2H, d, *J* = 5.7), 4.19 (2H, q, *J* = 7.1), 4.03 (2H,

d, *J* = 5.3), 1.27 (3H, t, *J* = 7.1); ^{13}C NMR (100 MHz; $CDCl_3$; Me_4Si) δ 171.7, 158.2, 149.9, 149.0, 141.1, 137.1, 128.7, 127.6, 122.0, 61.8, 44.5, 42.7, 14.6; HRMS (ES+) *m/z* 314.1502 $[M+H]^+$ $C_{17}H_{20}N_3O_3$ requires 314.1505 (Diff -0.8 ppm); Anal. Calcd. for $C_{17}H_{19}N_3O_3$: C, 65.16; H, 6.11; N, 13.41. Found C, 64.91; H, 6.07; N, 13.30.

Ethyl 2-(3-(3-(pyridin-3-yl)benzyl)ureido)acetate (7). The crude product was purified by flash column chromatography eluting with 70% EtOAc in hexane to 100% EtOAc to yield a white solid (183 mg, 0.58 mmol, 67%). M.p: 78 - 80°C; IR v_{max} (cm^{-1}) 1209 (C-O), 1568 (N-H), 1626 (amide C=O), 1736 (ester C=O), 3330 (N-H); ^{1}H NMR (400MHz; $CDCl_3$; Me_4Si; ppm) δ 8.76 (1H, s), 8.56 (1H, d, *J* = 4.9), 7.83 (1H, ap: dt, *J* = 7.9, 2.0), 7.45 (1H, ap: t, *J* = 1.8), 7.41 (1H, ap: dt, *J* = 7.8, 1.8), 7.37 (1H, ap: t, *J* = 7.4), 7.34 (1H, dd, *J* = 7.4, 4.8), 7.30 (1H, ap: dt, *J* = 7.4, 1.6), 5.72 (1H, t, *J* = 5.9), 5.54 (1H, t, *J* = 5.5), 4.41 (2H, d, *J* = 5.8), 4.13 (2H, q, *J* =7.2), 3.96 (2H, d, *J* = 5.4), 1.22 (3H, t, *J* = 7.1); ^{13}C NMR (100 MHz; $CDCl_3$; Me_4Si) δ 171.8, 158.6, 148.8, 148.6, 140.8, 138.4, 136.8, 134.9, 129.7, 127.6, 126.5, 126.3, 124.0, 61.7, 44.6, 42.7, 14.6; HRMS (ES+) *m/z* 336.1314 $[M+Na]^+$ $C_{17}H_{19}N_3O_3Na$ requires 336.1324 (Diff -3.0 ppm); Anal. Calcd. for $C_{17}H_{19}N_3O_3$: C, 65.16; H, 6.11; N, 13.41. Found C, 64.68; H, 6.09; N, 13.29.

Ethyl 2-(3-(3-(3-aminopyridin-4-yl)benzyl)ureido)acetate (8). The crude product was purified by flash column chromatography eluting with 100% EtOAc to 10% MeOH in EtOAc to yield a hygroscopic cream foam (304 mg, 0.93 mmol, 92%). IR v_{max} (cm^{-1}) 1191 (C-O), 1552 (N-H), 1634 (amide C=O), 1736 (ester C=O), 3326 (N-H); ^{1}H NMR (400MHz; $CDCl_3$; Me_4Si; ppm) δ 8.12 (1H, s), 8.02 (1H, d, *J* = 4.8), 7.42 (1H, ap: t, *J* = 7.9), 7.37 (1H, ap: t, *J* = 1.4), 7.33 (2H, ap: dd, *J* = 7.8, 1.4), 7.00 (1H, d, *J* = 4.9), 5.39 (1H, t, *J* = 5.5), 5.27 (1H, s), 4.42 (2H, d, *J* = 5.4), 4.16 (2H, q, *J* = 7.2), 3.98 (2H, d, *J* = 3.3), 1.26 (3H, t, *J* = 7.2); ^{13}C NMR (100 MHz; $CDCl_3$; Me_4Si) δ

171.7, 158.3, 140.7, 140.3, 140.3, 138.3, 137.6, 133.9, 129.8, 127.7, 127.6, 127.6, 124.6, 61.8, 44.7, 42.7, 14.5; HRMS (ES+) *m/z* 329.1616 $[M+H]^+$ $C_{17}H_{21}N_4O_3$ requires 329.1614 (Diff 0.7 ppm).

Ethyl ((4-acetamidobenzyl)carbamoyl)glycinate (9). The crude product was purified by flash column chromatography eluting with 50% EtOAc in hexane to 100% EtOAc to yield a beige foam (255 mg, 0.87 mmol, 96%). M.p: 171 - 173°C; IR v_{max} (cm^{-1}) 1203 (C-O), 1533 (N-H), 1581 (N-H), 1622 (amide C=O), 1685 (amide C=O), 1739 (ester C=O), 3321 (N-H), 3354 (N-H), 3379 (N-H); ^1H NMR (400MHz; DMSO; Me_4Si; ppm) δ 9.89 (1H, s), 7.49 (2H, d, *J* = 8.5), 7.15 (2H, d, *J* = 8.5), 6.61 (1H, t, *J* = 6.0), 6.26 (1H, t, *J* = 6.0), 4.14 (2H, d, *J* = 6.0), 4.08 (2H, q, *J* = 7.1), 3.77 (2H, d, *J* = 6.0), 2.02 (3H, s), 1.19 (3H, t, *J* = 7.1); ^{13}C NMR (100 MHz; DMSO; Me_4Si) δ 171.2, 168.1, 157.9, 137.9, 135.2, 127.4, 118.9, 60.2, 42.5, 41.6, 23.9, 14.1; HRMS (ES+) *m/z* 316.1263 $[M+Na]^+$ $C_{14}H_{19}N_3O_4Na$ requires 316.1273 (Diff -3.2 ppm); Anal. Calcd. for $C_{14}H_{19}N_3O_4$: C, 57.33; H, 6.53; N, 14.33. Found C, 57.45; H, 6.74; N, 13.45.

1-(4-Aminobenzyl)-3-(2-oxo-2-(pyrrolidin-1-yl)ethyl)urea (10). The crude product was purified by flash column chromatography eluting with 50% EtOAc in hexane to 100% EtOAc to yield an off white foam (140 mg, 0.61 mmol, 79%) IR v_{max} (cm^{-1}) 1638, 1655, 3299; ^1H NMR (400MHz; $(CD_3)_2SO$; Me_4Si; ppm) δ 6.81 (2H, d, *J* = 8.4 Hz), 6.43-6.39 (3H, m), 5.91 (1H, br t, *J* = 5.0 Hz), 4.82 (2H, br s), 3.92 (2H, d, *J* = 5.2 Hz), 3.71 (2H, d, *J* = 4.8 Hz), 3.29-3.19 (4H, m), 1.79 (2H, quintet, *J* = 6.8 Hz), 1.67 (2H, quintet, *J* = 6.8Hz); ^{13}C NMR (100 MHz; $(CD_3)_2SO$; Me_4Si) δ 169.2, 158.3, 143.2, 139.4, 136.2, 125.6, 50.7, 44.6, 43.2, 28.9; HRMS (ES+) *m/z* 277.1655 $[M+H]^+$ $C_{14}H_{21}N_4O_2$ requires 277.1659. Anal. Calcd. for $C_{14}H_{20}N_4O_2$: C, 60.85; H, 7.30; N, 20.28. Found C, 59.95; H, 7.12; N, 19.74.

tert-Butyl (4-(2-bromophenyl)-4-oxobutyl)carbamate (20a). A flame dried, Ar filled flask was charged with iPrMgCl.LiCl (0.68 ml, 0.89 mmol, 1.05 eq) and cooled to -15°C. 2-bromoiodobenzene (0.11 ml, 250 mg, 0.88 mmol, 1 eq) was added and the reaction mixture was allowed to stir for 30 mins at -10°C. Tert-butyl 2-oxopyrrolidine-1-carboxylate (179 mg, 0.97 mmol, 1.1 eq) was added and the reaction mixture was stirred at 0°C for 2 hrs. After this time, the reaction mixture was quenched with sat. NH_4Cl (10 ml) and extracted with EtOAc (3 x 10 ml). The combined organic layers were washed with water (10 ml) and brine (10 ml), dried over $MgSO_4$, filtered and concentrated *in vacuo*. The crude product was purified by flash column chromatography eluting with 5% EtOAc in hexane to 10% EtOAc in hexane to yield a colourless oil (91 mg, 0.27 mmol, 30%). ^{1}H NMR (400MHz; $CDCl_3$; Me_4Si; ppm) δ 7.60 (1H, d, *J* = 7.9), 7.39 (1H, dd, *J* = 7.9, 2.5), 7.35 (1H, dd, *J* = 7.7, 1.1), 7.30 (1H, dd, *J* = 7.9, 2.6), 4.93 (1H, s, minor rotamer), 4.71 (1H, s, major rotamer), 3.37 – 3.33 (2H, m, minor rotamer), 3.22 (2H, q, *J* = 6.1, major rotamer), 2.96 (2H, t, *J* = 7.0), 1.93 (2H, quintet, *J* = 7.0), 1.45 (9H, s, minor rotamer), 1.43 (9H, s, major rotamer); ^{13}C NMR (100 MHz; $CDCl_3$; Me_4Si) δ 203.8, 156.1, 155.7, 141.7, 135.4, 133.6, 131.5, 129.3, 128.3, 127.4, 123.5, 118.5, 79.2, 39.9, 38.8, 30.9, 28.4, 28.3, 24.3; LRMS (ES+) *m/z* 364.1 $[M+Na]^+$ $C_{15}H_{20}NO_3{}^{79}BrNa$ requires 364.1 (99%), *m/z* 366.0 $[M+Na]^+$ $C_{15}H_{20}NO_3{}^{81}BrNa$ requires 366.1 (100%);

tert-Butyl (4-(2-(methylthio)phenyl)-4-oxobutyl)carbamate (20b and 20c). Magnesium (1.00 g, 41.20 mmol, 10 eq) and iodine (single crystal) were stirred overnight under Ar in a flame dried flask at r.t. After this time, THF (10.3 ml, 0.4 M) was added to the activated magnesium. 2-bromothioanisole (0.55 ml, 837 mg, 4.12 mmol, 1 eq) was added at 0°C and the reaction mixture was allowed to warm to r.t. after 15 mins and refluxed for 2 hrs. After this time, the reaction mixture was allowed

to cool to r.t. Tert-butyl 2-oxopyrrolidine-1-carboxylate (555 mg, 3.00 mmol, 1 eq) was dissolved in THF (21 ml, 0.1 M) and cooled to -78°C. The aryl grignard (9 ml, 3.60 mmol, 1.2 eq) was added and allowed to stir for 15 mins before warming to 0°C and stirred for 30 mins. The reaction mixture was then warmed to r.t. and stirred overnight. After this time, the reaction mixture was quenched with sat. NH_4Cl (40 ml) and extracted with EtOAc (3 x 40 ml). The combined organic layers were dried over $MgSO_4$, filtered and concentrated *in vacuo*. The crude product was purified by flash column chromatography eluting with 100% hexane to 10% EtOAc in hexane to yield a white semi-solid (959 mg, 3.10 mmol, 36%). ^{1}H NMR (400MHz; $CDCl_3$; Me_4Si; ppm) δ 7.81 (1H, d, *J* = 7.7), 7.47 (1H, t, *J* = 7.7), 7.33 (1H, d, *J* = 7.9), 7.19 (1H, t, *J* = 7.5), 3.22 (2H, q, *J* = 7.0), 3.01 (2H, t, *J* = 7.0), 2.43 (3H, s), 1.94 (2H, quintet, *J* = 7.0), 1.42 (9H, s); ^{13}C NMR (100 MHz; $CDCl_3$; Me_4Si) δ 200.9, 156.1, 134.5, 129.5, 132.2, 130.1, 125.2, 123.6, 77.2, 40.1, 37.2, 28.4, 24.6, 16.0; HRMS (ES+) *m/z* 332.1298 $[M+Na]^+$ $C_{16}H_{23}NO_3SNa$ requires 332.1296 (Diff 0.5 ppm).

(*S*)-tert-Butyl (4-(2-bromophenyl)-4-hydroxybutyl)carbamate (21a). A solution of tert-butyl (4-(2-bromophenyl)-4-oxobutyl)carbamate (2.90 g, 8.48 mmol, 1 eq) in THF (12.7 ml, 0.67 M) was added dropwise to (*R*)-2-methyl-CBS-oxazaborolidine (0.25 ml, 236 mg, 0.85 mmol, 10 mol%) in 1M BH_3-DMS (8.48 ml, 8.48 mmol, 1 eq). The reaction mixture was stirred at r.t. for 3 hrs. After this time, the reaction mixture was quenched with 1M HCl (60 ml) and extracted with EtOAc (2 x 60 ml). The combined organic layers were dried over $MgSO_4$, filtered and concentrated *in vacuo*. The crude product was purified by flash column chromatography eluting with 10% EtOAc in hexane to 15% EtOAc in hexane to yield a colourless oil (2.81 g, 8.19 mmol, 97%). ^{1}H NMR (400MHz; CD_3OD; Me_4Si; ppm) δ 7.56 (1H, dd, *J* = 7.8, 1.5), 7.50 (1H, dd, *J* = 8.0, 1.0), 7.33 (1H, td, *J* = 7.7, 0.9), 7.12 (1H, td, *J* = 7.9, 1.7), 5.10 – 5.07 (1H, m),

4.63 (1H, br s), 3.28 – 3.23 (2H, m, minor rotamer), 3.19 – 3.11 (2H, m, major rotamer), 2.58 (1H, br s), 1.83 – 1.78 (4H, m, minor rotamer), 1.72 – 1.64 (4H, m, major rotamer), 1.43 (9H, s); ^{13}C NMR (100 MHz; $CDCl_3$; Me_4Si) δ 156.2, 143.8, 132.6, 128.8, 127.7, 127.3, 121.8, 79.3, 72.6, 40.3, 34.4, 28.4, 26.5; HRMS (ES+) *m/z* 366.0675 $[M+Na]^+$ $C_{15}H_{22}NO_3{}^{79}BrNa$ requires 366.0681 (100%) (Diff -1.6 ppm), *m/z* 368.0657 $[M+Na]^+$ $C_{15}H_{22}NO_3{}^{81}BrNa$ requires 368.0660 (98.5%) (Diff -0.9 ppm). HPLC on a chiral stationary phase revealed a 95:5 er with the first eluting peak at t_R = 6.14 min (major enantiomer) corresponding to (*S*)-**21a**, the second eluting peak at t_R = 6.97 min (minor enantiomer) corresponding to (*R*)-**21a**

(*S*)-tert-Butyl (4-hydroxy-4-(2-(methylthio)phenyl)butyl)carbamate (21b). A solution of tert-butyl (4-(2-(methylthio)phenyl)-4-oxobutyl)carbamate (825 mg, 2.67 mmol, 1 eq) in THF (4 ml, 0.67 M) was added dropwise to (*R*)-2-methyl-CBS-oxazaborolidine (1 M in toluene) (0.27 ml, 0.27 mmol, 10 mol%) in 1M BH_3-DMS (2.67 ml, 2.67 mmol, 1 eq). The reaction mixture was stirred at r.t. for 3 hrs. After this time, the reaction mixture was quenched with 1M HCl (40 ml) and extracted with EtOAc (2 x 40 ml). The combined organic layers were dried over $MgSO_4$, filtered and concentrated *in vacuo*. The crude product was purified by flash column chromatography eluting with 10% EtOAc in hexane to 20% EtOAc in hexane to yield a colourless oil (761 mg, 2.45 mmol, 92%). $[\alpha]_D^{25.4}$ -41.6 (c 0.01, CH_3OH); ^{1}H NMR (400MHz; $CDCl_3$; Me_4Si; ppm) δ 7.48 (1H, d, *J* = 7.4), 7.25 – 7.23 (2H, m), 7.20 (1H, dt, *J* = 7.6, 2.9), 5.13 (1H, dd, *J* = 7.6, 4.4), 4.67 (1H, s), 3.23 – 3.13 (2H, m), 2.46 (3H, s), 1.78 – 1.58 (4H, m), 1.43 (9H, s); ^{13}C NMR (100 MHz; $CDCl_3$; Me_4Si) δ 156.1, 143.0, 135.3, 127.9, 126.3, 125.6, 125.5, 79.1, 70.4, 40.3, 34.7, 28.4, 26.5, 16.4; LRMS (ES+) *m/z* 334.1 $[M+Na]^+$ $C_{16}H_{25}NO_3SNa$ requires 334.1. HPLC on a chiral stationary phase revealed a 95:5 er with the first eluting peak at t_R = 8.87 min

(major enantiomer) corresponding to (*S*)-**21b**, the second eluting peak at t_R = 10.66 min (minor enantiomer) corresponding to (*R*)-**21c**.**(*R*)-tert-Butyl (4-hydroxy-4-(2-(methylthio)phenyl)butyl)carbamate (21c).** A solution of tert-butyl (4-(2-(methylthio)phenyl)-4-oxobutyl)carbamate (825 mg, 2.67 mmol, 1 eq) in THF (4 ml, 0.67 M) was added dropwise to (*S*)-2-methyl-CBS-oxazaborolidine (1 M in toluene) (0.27 ml, 0.27 mmol, 10 mol%) in 1M BH_3-DMS (2.67 ml, 2.67 mmol, 1 eq). The reaction mixture was stirred at r.t. for 3 hrs. After this time, the reaction mixture was quenched with 1N HCl (40 ml) and extracted with EtOAc (2 x 40 ml). The combined organic layers were dried over $MgSO_4$, filtered and concentrated *in vacuo*. The crude product was purified by flash column chromatography eluting with 10% EtOAc in hexane to 15% EtOAc in hexane to yield a colourless oil (728 mg, 2.34 mmol, 88%). $[\alpha]_D^{25.1}$ +26.0 (c 0.01, CH_3OH); ^{1}H NMR (400MHz; $CDCl_3$; Me_4Si; ppm) δ 7.48 (1H, d, *J* = 7.5), 7.25 – 7.23 (2H, m), 7.20 (1H, dt, *J* = 7.5, 3.1), 5.13 (1H, dd, *J* = 7.5, 4.5), 4.64 (1H, s), 3.25 – 3.13 (2H, m), 2.47 (3H, s), 1.78 – 1.61 (4H, m), 1.43 (9H, s); ^{13}C NMR (100 MHz; $CDCl_3$; Me_4Si) δ 156.1, 143.0, 135.3, 127.9, 126.4, 125.6, 125.6, 79.1, 70.5, 40.3, 34.7, 28.4, 26.6, 16.4; LRMS (ES+) *m/z* 334.1 $[M+Na]^+$ $C_{16}H_{25}NO_3SNa$ requires 334.1. HPLC on a chiral stationary phase revealed a 95:5 er with the first eluting peak at t_R = 8.73 min (minor enantiomer) corresponding to (*S*)-**21b**, the second eluting peak at t_R = 10.47 min (major enantiomer) corresponding to (*R*)-**21c**.

(*S*)-1-(2-Bromophenyl)-4-((tert-butoxycarbonyl)amino)butyl methanesulfonate (22a). (*S*)-tert-butyl (4-(2-bromophenyl)-4-hydroxybutyl)carbamate (2.81 g, 8.19 mmol, 1 eq) was dissolved in DCM (81.9 ml, 0.1 M) and cooled to 0°C. NEt_3 (4.57 ml, 3.31 g, 32.76 mmol, 4 eq) and methanesulfonyl chloride (1.90 ml, 2.81 g, 24.57 mmol, 3 eq) were added to the reaction mixture and stirred at 0°C for 15 mins before

warming to r.t. and stirred for 3 hrs. After this time, the reaction mixture was concentrated *in vacuo*. The residue was dissolved in EtOAc (60 ml) and washed with 1N HCl (50 ml), $NaHCO_3$ (50 ml), water (50 ml) and brine (50 ml). The organic layer was dried over $MgSO_4$, filtered and concentrated *in vacuo*. The crude product was purified by flash column chromatography eluting with 1% EtOAc in hexane to 5% EtOAc in hexane to yield a pale yellow oil (1.97 g, 4.68 mmol, 57%). ^{1}H NMR (400MHz; $CDCl_3$; Me_4Si; ppm) δ 7.51 (1H, dd, *J* = 7.9, 1.0), 7.25 (1H, t, *J* = 7.4), 7.14 (1H, d, *J* = 7.8), 7.08 (1H, t, *J* = 7.4), 5.22 (1H, d, *J* = 7.5, minor rotamer), 5.12 (1H, dd, *J* = 7.8, 4.4, major rotamer), 3.71 – 3.60 (2H, m, major rotamer), 3.55 – 3.49 (2H, m, minor rotamer), 2.44 – 2.32 (1H, m), 1.92 – 1.85 (3H, m, major rotamer), 1.82 – 1.75 (3H, m, minor rotamer), 1.60 (3H, s, minor rotamer), 1.46 (9H, s, minor rotamer), 1.44 (3H, s, major rotamer), 1.18 (9H, s, major rotamer); ^{13}C NMR (100 MHz; $CDCl_3$; Me_4Si) δ 154.3, 143.8, 132.8, 132.6, 129.6, 128.6, 128.0, 128.0, 127.3, 126.5, 121.9, 79.3, 52.6, 47.3, 36.6, 34.0, 28.4, 28.1, 23.0; HRMS (ES+) *m/z* 348.0569 $[M\text{-}OMs+Na]^+$ $C_{15}H_{20}NO_2{}^{79}BrNa$ requires 348.0575 (100%) (Diff -1.8 ppm), *m/z* 350.0548 $[M\text{-}OMs+Na]^+$ $C_{15}H_{20}NO_2{}^{81}BrNa$ requires 350.0555 (99.7%) (Diff -1.9 ppm).

(*S*)-4-((tert-Butoxycarbonyl)amino)-1-(2-(methylthio)phenyl)butyl methanesulfonate (22b). (*S*)-tert-butyl (4-hydroxy-4-(2-(methylthio)phenyl)butyl)carbamate (761 mg, 2.45 mmol, 1 eq) was dissolved in DCM (25 ml, 0.1 M) and cooled to 0°C. NEt_3 (1.37 ml, 992 mg, 9.80 mmol, 4 eq) and methanesulfonyl chloride (0.57 ml, 842 mg, 7.35 mmol, 3 eq) were added to the reaction mixture and stirred at 0°C for 15 mins before warming to r.t. and stirred for 3 hrs. After this time, the reaction mixture was concentrated *in vacuo*. The residue was dissolved in EtOAc (40 ml) and washed with 1N HCl (30 ml), $NaHCO_3$ (30 ml), water

(30 ml) and brine (30 ml). The organic layer was dried over $MgSO_4$, filtered and concentrated *in vacuo*. The crude product was purified by flash column chromatography eluting with 1% EtOAc in hexane to 5% EtOAc in hexane to yield a colourless oil (542 mg, 1.39 mmol, 57%). ^{1}H NMR (400MHz; $CDCl_3$; Me_4Si; ppm) δ 7.23 (1H, s), 7.19 (1H, d, *J* = 8.4), 7.14 (1H, d, *J* = 8.4), 7.10 (1H, s), 5.16 (1H, s), 3.67 – 3.60 (2H, m), 2.47 (3H, s), 2.35 – 2.28 (1H, m), 1.86 – 1.77 (3H, m), 1.46 (3H, s), 1.17 (9H, s). ^{13}C NMR (100 MHz; $CDCl_3$; Me_4Si) δ 154.5, 143.3, 135.0, 127.0, 126.6, 125.2, 124.9, 79.1, 58.6, 50.9, 47.1, 34.1, 28.1, 23.1, 16.6; LRMS (ES+) *m/z* 316.1 $[M\text{-}OMs+Na]^+$ $C_{16}H_{23}NO_2SNa$ requires 316.1.

(*R*)-4-((tert-Butoxycarbonyl)amino)-1-(2-(methylthio)phenyl)butyl methanesulfonate (22c). (*R*)-tert-butyl (4-hydroxy-4-(2-(methylthio)phenyl)butyl)carbamate (728 mg, 2.34 mmol, 1 eq) was dissolved in DCM (23 ml, 0.1 M) and cooled to 0°C. NEt_3 (1.30 ml, 947 mg, 9.36 mmol, 4 eq) and methanesulfonyl chloride (0.54 ml, 804 mg, 7.02 mmol, 3 eq) were added to the reaction mixture and stirred at 0°C for 15 mins before warming to r.t. and stirred for 3 hrs. After this time, the reaction mixture was concentrated *in vacuo*. The residue was dissolved in EtOAc (40 ml) and washed with 1N HCl (30 ml), $NaHCO_3$ (30 ml), water (30 ml) and brine (30 ml). The organic layer was dried over $MgSO_4$, filtered and concentrated *in vacuo*. The crude product was purified by flash column chromatography eluting with 2% EtOAc in hexane to 4% EtOAc in hexane to yield a colourless oil (505 mg, 1.30 mmol, 55%). ^{1}H NMR (400MHz; $CDCl_3$; Me_4Si; ppm) δ 7.23 (1H, s), 7.19 (1H, d, *J* = 8.2), 7.13 (1H, d, *J* = 8.2), 7.10 (1H, s), 5.16 (1H, s), 3.67 – 3.59 (2H, m), 2.47 (3H, s), 2.35 – 2.28 (1H, m), 1.87 – 1.77 (3H, m), 1.46 (3H, s), 1.17 (9H, s). ^{13}C NMR (100 MHz; $CDCl_3$; Me_4Si) δ 154.5, 143.3, 135.0, 127.0,

126.6, 125.2, 124.9, 79.1, 58.6, 50.9, 47.1, 34.1, 28.1, 23.1, 16.6; LRMS (ES+) *m/z* 316.1 $[M\text{-}OMs+Na]^+$ $C_{16}H_{23}NO_2SNa$ requires 316.1.

(*R*)-2-(2-Bromophenyl)pyrrolidine (23a). (*S*)-1-(2-bromophenyl)-4-((tert-butoxycarbonyl)amino)butyl methanesulfonate (985 mg, 2.34 mmol, 1 eq) was dissolved in DCM:TFA (23.4 ml, 5:1, 0.1 M) and stirred at r.t. for 2 hrs. After this time, the reaction mixture was concentrated *in vacuo*. The yellow oil was dissolved in 1M NaOH (7.02 ml, 7.02 mmol, 3 eq) in MeOH (16.38 ml, 0.1 M total volume). The reaction mixture was stirred overnight at r.t. After this time, the reaction mixture was concentrated *in vacuo*. The residue was neutralised with 1M HCl and washed with EtOAc (2 x 50 ml). The combined organic layers were dried over $MgSO_4$, filtered and concentrated *in vacuo* to yield a yellow solid that required no further purification (802 mg, 3.56 mmol, Quantitative). ^{1}H NMR (400MHz; $CDCl_3$; Me_4Si; ppm) δ 7.54 (2H, dd, *J* = 7.7, 3.6), 7.33 – 7.28 (1H, m), 7.16 (1H, t, *J* = 7.6), 4.88 (1H, t, *J* = 8.1), 3.41 – 3.35 (1H, m), 3.31 – 3.23 (1H, m), 2.47 – 2.40 (1H, m), 2.20 – 2.13 (1H, m), 2.10 – 1.95 (2H, m); ^{13}C NMR (100 MHz; $CDCl_3$; Me_4Si) δ 135.8, 133.2, 130.1, 128.1, 127.6, 123.9, 61.6, 45.7, 32.0, 24.0; HRMS (ES+) *m/z* 226.0226 $[M+H]^+$ $C_{10}H_{13}N^{79}Br$ requires 226.0231 (97.4%) (Diff -2.4 ppm), *m/z* 228.0206 $[M+H]^+$ $C_{10}H_{13}N^{81}Br$ requires 228.0211 (100%) (Diff -2.1 ppm).

(*R*)-2-(2-(Methylthio)phenyl)pyrrolidine (23b). (*S*)-4-((tert-butoxycarbonyl)amino)-1-(2-(methylthio)phenyl)butyl methanesulfonate (542 mg, 1.39 mmol, 1 eq) was dissolved in DCM:TFA (13.9 ml, 5:1, 0.1 M) and stirred at r.t. for 2 hrs. After this time, the reaction mixture was concentrated *in vacuo*. The pale yellow oil was dissolved in 1M NaOH (4.17 ml, 4.17 mmol, 3 eq) in MeOH (9.73 ml, 0.1 M total volume). The reaction mixture was stirred overnight at r.t. After this time, the reaction mixture was concentrated *in vacuo*. The residue was neutralised with 1M HCl and

washed with EtOAc (2 x 40 ml). The combined organic layers were dried over $MgSO_4$, filtered and concentrated *in vacuo* to yield an orange oil that required no further purification (181 mg, 0.94 mmol, 68%). ^{1}H NMR (400MHz; $CDCl_3$; Me_4Si; ppm) δ 7.51 (1H, d, *J* = 7.4), 7.23 (2H, s), 7.14 (1H, t, *J* = 7.3), 4.56 (1H, t, *J* = 7.3), 3.20 (1H, q, *J* = 7.8), 3.05 (1H, q, *J* = 7.9), 2.46 (3H, s), 2.30 – 2.20 (1H, m), 1.93 – 1.85 (2H, m), 1.66 – 1.58 (1H, m); ^{13}C NMR (100 MHz; $CDCl_3$; Me_4Si) δ 142.0, 136.6, 127.4, 125.9, 125.7, 125.3, 58.9, 46.7, 32.7, 25.3, 16.2; HRMS (CI+) *m/z* 194.1005 $[M+H]^+$ $C_{11}H_{16}NS$ requires 194.0998 (Diff 3.5 ppm).

(*S*)-2-(2-(Methylthio)phenyl)pyrrolidine (23c). (*R*)-4-((tert-butoxycarbonyl)amino)-1-(2-(methylthio)phenyl)butyl methanesulfonate (505 mg, 1.30 mmol, 1 eq) was dissolved in DCM:TFA (13.0 ml, 5:1, 0.1 M) and stirred at r.t. for 2 hrs. After this time, the reaction mixture was concentrated *in vacuo*. The pale orange oil was dissolved in 1M NaOH (3.90 ml, 3.90 mmol, 3 eq) in MeOH (9.10 ml, 0.1 M total volume). The reaction mixture was stirred overnight at r.t. After this time, the reaction mixture was concentrated *in vacuo*. The residue was neutralised with 1M HCl and washed with EtOAc (2 x 40 ml). The combined organic layers were dried over $MgSO_4$, filtered and concentrated *in vacuo* to yield a pale yellow oil that required no further purification (250 mg, 1.29 mmol, 100%). ^{1}H NMR (400MHz; $CDCl_3$; Me_4Si; ppm) δ 8.14 (1H, br s), 7.51 (1H, d, *J* = 7.4), 7.22 (2H, s), 7.16 (1H, t, *J* = 7.3), 4.62 (1H, t, *J* = 7.4), 3.27 – 3.23 (3H, m), 3.09 (1H, q, *J* = 7.4), 2.47 (3H, s), 2.34 – 2.26 (1H, m), 1.97 – 1.89 (1H, m), 1.73 – 1.64 (1H, m); ^{13}C NMR (100 MHz; $CDCl_3$; Me_4Si) δ 141.1, 136.7, 127.6, 126.1, 125.8, 125.4, 59.0, 46.6, 32.6, 25.2, 16.4; LRMS (CI+) *m/z* 194.1 $[M+H]^+$ $C_{11}H_{16}NS$ requires 194.1.

(*R*)-tert-butyl (2-(2-(2-bromophenyl)pyrrolidin-1-yl)-2-oxoethyl)carbamate (24a). (*R*)-2-(2-bromophenyl)pyrrolidine (802 mg, 3.56 mmol, 1 eq), Boc-Glycine (748 mg,

4.27 mmol, 1.2 eq) and HATU (1.76 g, 4.63 mmol, 1.3 eq) were dissolved in DMF (17.8 ml, 0.2 M). DIPEA (0.93 ml, 690 mg, 5.34 mmol, 1.5 eq) was added and the reaction mixture was stirred at room temperature overnight. After this time, the reaction mixture was diluted with EtOAc (40 ml) and washed with $NaHCO_3$ (3 x 40 ml), water (40 ml) and brine (40 ml). The organic layer was dried over $MgSO_4$, filtered and concentrated *in vacuo*. The crude product was purified by flash column chromatography eluting with 15% EtOAc in hexane to 20% EtOAc in hexane to yield a colourless oil (862 mg, 2.26 mmol, 63%). ^{1}H NMR (400MHz; $CDCl_3$; Me_4Si; ppm) δ 7.57 (1H, d, *J* = 8.0, major rotamer), 7.55 (1H, dd, *J* = 8.0, 0.8, minor rotamer), 7.28 (1H, t, *J* = 7.5, major rotamer), 7.23 (1H, t, *J* = 7.5, minor rotamer), 7.15 (1H, t, *J* = 7.8, major rotamer), 7.09 (1H, td, *J* = 7.8, 1.5, minor rotamer), 7.03 (1H, d, *J* = 7.6, major rotamer), 6.94 (1H, dd, *J* = 7.7, 1.2, minor rotamer), 5.42 (1H, dd, *J* = 8.5, 2.5, major rotamer), 5.35 (1H, br s), 5.20 (1H, d, *J* = 8.1, minor rotamer), 4.03 – 4.00 (1H, m, major rotamer), 3.98 – 3.93 (1H, m, minor rotamer), 3.88 – 3.83 (2H, m, minor rotamer), 3.79 – 3.70 (2H, m, major rotamer), 3.59 (1H, ap: q, *J* = 7.9, minor rotamer), 3.26 (1H, dd, *J* = 17.3, 3.7, major rotamer), 2.48 – 2.39 (1H, m, major rotamer), 2.36 – 2.29 (1H, m, minor rotamer), 2.03 – 1.94 (2H, m), 1.92 – 1.88 (1H, m, major rotamer), 1.87 – 1.81 (1H, m, minor rotamer), 1.43 (9H, s, minor rotamer), 1.40 (9H, s, major rotamer); ^{13}C NMR (100 MHz; $CDCl_3$; Me_4Si) δ 168.0, 167.0, 155.9, 155.7, 141.0, 140.6, 133.6, 133.3, 129.2, 128.5, 127.9, 127.4, 126.1, 125.9, 122.1, 121.9, 79.6, 79.5, 61.2, 60.5, 47.8, 46.9, 43.2, 42.8, 32.3, 28.3, 23.4; HRMS (ES+) *m/z* 405.0783 $[M+Na]^+$ $C_{17}H_{23}N_2O_3{}^{79}BrNa$ requires 405.0790 (100%) (Diff -1.7 ppm), *m/z* 407.0778 $[M+Na]^+$ $C_{17}H_{23}N_2O_3{}^{81}BrNa$ requires 407.0769 (95.9%) (Diff 2.1 ppm).

(R)-tert-butyl (2-(2-(2-(methylthio)phenyl)pyrrolidin-1-yl)-2-oxoethyl)carbamate (24b). (*R*)-2-(2-(methylthio)phenyl)pyrrolidine (100 mg, 0.52 mmol, 1 eq), *N*-(tert-butoxycarbonyl) glycine (109 mg, 0.62 mmol, 1.2 eq) and HATU (259 mg, 0.68 mmol, 1.3 eq) were dissolved in DMF (2.6 ml, 0.2 M). DIPEA (0.14 ml, 101 mg, 0.78 mmol, 1.5 eq) was added and the reaction mixture was stirred at room temperature overnight. After this time, the reaction mixture was diluted with EtOAc (10 ml) and washed with $NaHCO_3$ (3 x 10 ml), water (10 ml) and brine (10 ml). The organic layer was dried over $MgSO_4$, filtered and concentrated in vacuo. The crude product was purified by flash column chromatography eluting with 30% EtOAc in hexane to 50% EtOAc in hexane to yield a colourless oil (178 mg, 0.51 mmol, 98%). ^{1}H NMR (400MHz; $CDCl_3$; Me_4Si; ppm) δ 7.28 – 7.25 (2H, m, major rotamer), 7.20 (2H, td, *J* = 7.9, 1.1, minor rotamer), 7.14 – 7.08 (1H, m), 6.97 (1H, d, *J* = 7.6, major rotamer), 6.91 (1H, d, *J* = 7.5, minor rotamer), 5.50 (1H, dd, *J* = 8.2, 3.0, minor rotamer), 5.46 (1H, s, minor rotamer), 5.37 (1H, s, major rotamer), 5.24 (1H, d, *J* = 7.7, major rotamer), 4.01 (1H, ap: t, *J* = 3.5, minor rotamer), 3.96 (1H, dd, *J* = 17.5, 5.3, major rotamer), 3.86 – 3.81 (1H, m), 3.77 – 3.68 (1H, m), 3.57 (1H, dd, *J* = 7.9, minor rotamer), 3.24 (1H, dd, *J* = 17.4, 3.6, major rotamer), 2.52 (3H, s, major rotamer), 2.50 (3H, s, minor rotamer), 2.38 – 2.33 (1H, m, major rotamer), 2.31 – 2.23 (1H, m, minor rotamer), 2.02 – 1.96 (3H, m, minor rotamer), 1.93 – 1.84 (3H, m, major rotamer), 1.43 (9H, s, minor rotamer), 1.39 (9H, s, major rotamer); ^{13}C NMR (100 MHz; $CDCl_3$; Me_4Si) δ 167.9, 155.7, 140.6, 139.4, 135.7, 135.3, 128.1, 127.5, 127.1, 126.1, 125.3, 125.2, 124.5, 124.4, 79.5, 79.4, 59.0, 58.0, 47.9, 46.7, 43.2, 42.8, 38.6, 34.1, 32.3, 28.4, 23.7, 16.5, 16.0; HRMS (ES+) *m/z* 373.1557 $[M+Na]^+$ $C_{18}H_{26}N_2O_3SNa$ requires 373.1562 (Diff -1.3 ppm).

***tert*-butyl ((*S*)-4-(methylthio)-1-((*R*)-2-(2-(methylthio)phenyl)pyrrolidin-1-yl)-1-oxobutan-2-yl)carbamate (25b).** (*R*)-2-(2-(methylthio)phenyl)pyrrolidine (181 mg, 0.94 mmol, 1 eq), Boc-L-methionine (282 mg, 1.13 mmol, 1.2 eq) and HATU (464 mg, 1.22 mmol, 1.3 eq) were dissolved in DMF (4.7 ml, 0.2 M). DIPEA (0.25 ml, 182 mg, 1.41 mmol, 1.5 eq) was added and the reaction mixture was stirred at room temperature overnight. After this time, the reaction mixture was diluted with EtOAc (20 ml) and washed with $NaHCO_3$ (3 x 20 ml), water (20 ml) and brine (20 ml). The organic layer was dried over $MgSO_4$, filtered and concentrated *in vacuo*. The crude product was purified by flash column chromatography eluting with 15% EtOAc in hexane to 20% EtOAc in hexane to yield a colourless oil as a mixture of 2 rotamers in approximately a 2:1 ratio (175 mg, 0.41 mmol, 44%). ^{1}H NMR (400MHz; $CDCl_3$; Me_4Si; ppm) δ 7.26 (1H, dd, *J* = 7.3, 3.1), 7.20 – 7.13 (1H, m), 7.06 (1H, t, *J* = 7.6), 6.99 (1H, q, *J* = 7.6), 5.64 (1H, d, *J* = 6.8, minor rotamer), 5.47 (1H, dd, *J* = 8.1, 2.2, major rotamer), 5.26 (1H, ap. d, *J* = 8.9, major rotamer), 4.70 (1H, ap. q, *J* = 8.2, minor rotamer), 4.26 (1H, br s, minor rotamer), 4.17 (1H, br s, major rotamer), 3.75 (2H, t, *J* = 8.8, major rotamer), 2.58 (2H, t, *J* = 7.1, minor rotamer), 2.53 (3H, s, major rotamer), 2.49 (3H, s, minor rotamer), 2.39 – 2.17 (2H, m), 2.12 (3H, s, major rotamer), 2.03 – 1.81 (6H, m), 1.68 (3H, s, minor rotamer), 1.45 (9H, s, major rotamer), 1.43 (9H, s, minor rotamer); ^{13}C NMR (100 MHz; $CDCl_3$; Me_4Si) δ 171.7, 170.3, 155.9, 155.4, 140.7, 135.8, 135.2, 128.1, 127.3, 127.2, 126.5, 125.7, 125.4, 125.0, 124.4, 79.8, 79.5, 59.0, 58.9, 52.5, 51.2, 47.7, 47.5, 33.9, 32.9, 32.5, 32.0, 30.3, 30.0, 28.4, 28.3, 23.4, 22.6, 16.6, 15.6, 15.1; HRMS (ES+) *m/z* 447.1748 $[M+Na]^+$ $C_{21}H_{32}N_2O_3S_2Na$ requires 447.1752 (Diff -0.9 ppm).

***tert*-butyl ((*S*)-4-(methylthio)-1-((*S*)-2-(2-(methylthio)phenyl)pyrrolidin-1-yl)-1-oxobutan-2-yl)carbamate (25c).** (*S*)-2-(2-(methylthio)phenyl)pyrrolidine (250 mg,

1.29 mmol, 1 eq), Boc-L-methionine (386 mg, 1.55 mmol, 1.2 eq) and HATU (639 mg, 1.68 mmol, 1.3 eq) were dissolved in DMF (6.5 ml, 0.2 M). DIPEA (0.34 ml, 251 mg, 1.94 mmol, 1.5 eq) was added and the reaction mixture was stirred at room temperature overnight. After this time, the reaction mixture was diluted with EtOAc (20 ml) and washed with $NaHCO_3$ (3 x 20 ml), water (20 ml) and brine (20 ml). The organic layer was dried over $MgSO_4$, filtered and concentrated *in vacuo*. The crude product was purified by flash column chromatography eluting with 10% EtOAc in hexane to 15% EtOAc in hexane to yield a colourless oil as a mixture of 2 rotamers in approximately a 2:1 ratio (264 mg, 0.62 mmol, 48%). ^{1}H NMR (400MHz; $CDCl_3$; Me_4Si; ppm) δ 7.27 (1H, d, *J* = 7.6), 7.20 (1H, t, *J* = 7.3), 7.10 (1H, t, *J* = 7.4), 6.92 (1H, d, *J* = 7.5), 5.52 (1H, dd, *J* = 8.1, 4.1, major rotamer), 5.36 (1H, d, *J* = 8.7, major rotamer), 5.24 (1H, d, *J* = 7.2, minor rotamer), 4.72 (1H, ap. q, *J* = 8.1, major rotamer), 4.03 (1H, ap. td, *J* = 8.1, 4.7, minor rotamer), 3.88 (2H, t, *J* = 6.9, major rotamer), 3.63 (1H, q, *J* = 8.9, minor rotamer), 2.54 (2H, t, *J* = 8.2, minor rotamer), 2.50 (3H, s), 2.44 – 2.27 (2H, m), 2.13 (3H, s, major rotamer), 2.10 (3H, s, minor rotamer), 2.06 – 1.97 (2H, m), 1.91 – 1.78 (4H, m), 1.43 (9H, s, major rotamer), 1.28 (9H, s, minor rotamer); ^{13}C NMR (100 MHz; $CDCl_3$; Me_4Si) δ 171.1, 170.2, 155.5, 154.3, 141.3, 135.6, 135.3, 128.1, 127.5, 127.3, 126.4, 125.4, 125.2, 124.8, 124.0, 79.7, 79.0, 58.7, 58.5, 51.6, 51.0, 48.0, 47.4, 34.1, 33.9, 32.9, 32.5, 30.2, 30.0, 28.4, 28.2, 24.2, 21.4, 16.6, 16.2, 15.7, 15.6; HRMS (ES+) *m/z* 447.1750 $[M+Na]^+$ $C_{21}H_{32}N_2O_3S_2Na$ requires 447.1752 (Diff -0.5 ppm).

(*R*)-1-(4-Aminobenzyl)-3-(2-oxo-2-(2-phenylpyrrolidin-1-yl)ethyl)urea (11). The crude product was purified by flash column chromatography eluting with 50% EtOAc in hexane to yield a white foam as a mixture of 2 rotamers in approximately a 1:1 ratio (292 mg, 0.83 mmol, 74%). ^{1}H NMR (400MHz; $(CD_3)_2SO$; Me_4Si; ppm) δ 7.39-

7.35 (1H, m), 7.30-7.26 (2H, m), 7.20-7.15 (3H, m), 6.90-6.84 (2H, m), 6.49-6.44 (3H, m), 6.00-5.92 (1H, m), 5.09-5.04 (1H, m), 4.92 (2H, br s), 4.01-3.94 (3H, m), 3.90-3.84 (1H, m, 1 rotamer), 3.75-3.72 (1H, m, 1 rotamer), 3.67-3.62 (1H, m, 1 rotamer), 3.58-3.51 (1H, m), 3.17-3.11 (1H, m, 1 rotamer), 2.40-2.28 (1H, m, 1 rotamer), 2.24-2.15 (1H, m, 1 rotamer), 1.95-1.70 (3H, m), ^{13}C NMR (100 MHz; $(CD_3)_2SO$; Me_4Si) δ 168.7, 168.2, 158.3, 158.1, 147.8, 147.8, 144.0, 143.8, 129.2, 128.5, 128.5, 127.9, 127.8, 127.5, 126.8, 125.9, 125.8, 114.1, 114.0, 60.5, 60.1, 47.3, 46.2, 43.2, 43.1, 42.8, 42.7, 36.4, 34.1, 23.5, 21.5, HRMS (ES+) *m/z* 375.1791 $[M+Na]^+$ $C_{20}H_{24}N_4NaO_2$ requires 375.1797. Anal. Calcd. for $C_{20}H_{24}N_4O_2$: C, 68.16; H, 6.86; N, 15.90. Found C, 67.77; H, 6.82; N, 15.95.

(R)-1-(4-Aminobenzyl)-3-(2-(2-(2-(methylthio)phenyl)pyrrolidin-1-yl)-2-oxoethyl)urea (12). The crude product was purified by flash column chromatography eluting with 50% EtOAc in hexane to yield a pale yellow oil as a mixture of 2 rotamers in approximately a 2:1 ratio (62 mg, 0.11 mmol, 26%). ^{1}H NMR (400MHz; $CDCl_3$; Me_4Si; ppm) δ 7.25 – 7.23 (1H, m), 7.21 – 7.15 (1H, m), 7.11 – 7.07 (1H, m), 7.04 (2H, ap: t, *J* = 8.2), 6.86 (1H, d, *J* = 7.5), 6.60 (2H, dd, *J* = 8.3, 2.5), 5.83 (1H, ap: q, *J* = 4.3, major rotamer), 5.78 (1H, ap: q, *J* = 4.2, minor rotamer), 5.45 – 5.41 (1H, m), 5.25 (1H, dd, *J* = 7.8, 1.4), 4.21 (2H, d, *J* = 5.6, minor rotamer), 4.18 – 4.15 (2H, m, major rotamer), 4.13 – 4.09 (2H, m, major rotamer), 4.06 (2H, d, *J* = 5.0, minor rotamer), 3.75 (1H, ddd, *J* = 10.5, 10.5, 5.7, major rotamer), 3.60 – 3.55 (1H, m, minor rotamer), 3.41 – 3.35 (1H, m, minor rotamer), 3.30 (1H, dd, *J* = 17.7, 3.0, major rotamer), 2.52 (3H, s, major rotamer), 2.43 (3H, s, minor rotamer), 2.34 – 2.17 (1H, m), 1.99 – 1.92 (2H, m, minor rotamer), 1.88 – 1.83 (2H, m, major rotamer), 1.78 – 1.74 (1H, m); ^{13}C NMR (100 MHz; $CDCl_3$; Me_4Si) δ 169.2, 168.0, 158.0, 158.0, 145.5, 145.5, 140.2, 139.5, 135.7, 135.3, 129.4, 128.9,

128.9, 128.1, 127.5, 126.6, 126.6, 125.3, 125.2, 124.5, 124.3, 115.2, 115.1, 59.0, 58.2, 47.3, 46.8, 44.1, 44.0, 43.2, 42.7, 34.1, 32.2, 23.5, 21.3, 16.2, 16.2; HRMS (ES+) *m/z* 421.1670 $[M+Na]^+$ $C_{21}H_{26}N_4O_2SNa$ requires 421.1674.

(*R*)-1-(4-Aminobenzyl)-3-(2-(2-(2-bromophenyl)pyrrolidin-1-yl)-2-oxoethyl)urea (13). The crude product was purified by flash column chromatography eluting with 100% EtOAc to yield a cream foam (428 mg, 1.00 mmol, 88%). ^{1}H NMR (400MHz; $CDCl_3$; Me_4Si; ppm) δ 7.56 (1H, dd, *J* = 7.9, 1.0, major rotamer), 7.50 (1H, d, *J* = 7.9, minor rotamer), 7.26 – 7.18 (1H, m), 7.16 – 7.11 (1H, m, major rotamer), 7.04 (2H, d, *J* = 7.8), 7.03 – 7.01 (1H, m, minor rotamer), 6.92 (1H, t, *J* = 8.0), 6.60 (2H, d, *J* = 7.8), 5.69 (1H, dd, *J* = 9.1, 4.9), 5.37 – 5.33 (1H, m, minor rotamer), 5.29 (1H, t, *J* = 5.2, major rotamer), 5.20 – 5.15 (1H, m), 4.20 (2H, d, minor rotamer, *J* = 5.5), 4.18 – 4.16 (2H, m, major rotamer), 4.12 (1H, d, minor rotamer, *J* = 4.5), 4.09 (1H, d, *J* = 5.3, major rotamer), 4.07 (1H, d, *J* = 4.4, minor rotamer), 4.05 (1H, d, *J* = 5.3, major rotamer), 3.79 – 3.74 (2H, m, minor rotamer), 3.61 – 3.55 (2H, m, major rotamer), 3.46 – 3.40 (1H, m, minor rotamer), 3.31 (1H, dd, *J* = 17.5, 3.6, major rotamer), 2.41 – 2.24 (3H, m, minor rotamer), 1.97 – 1.87 (3H, m, major rotamer), 1.83 – 1.70 (2H, m); ^{13}C NMR (100 MHz; $CDCl_3$; Me_4Si) δ 169.3, 168.2, 158.0, 157.9, 145.6, 145.5, 140.9, 140.5, 133.6, 133.2, 129.5, 129.2, 128.9, 128.8, 128.5, 127.8, 127.4, 126.1, 125.9, 122.0, 122.0, 115.2, 115.1, 61.2, 60.7, 47.6, 47.0, 44.2, 44.0, 43.1, 42.7, 34.2, 32.2, 23.3; HRMS (ES+) *m/z* 453.0897 $[M+Na]^+$ $C_{20}H_{23}N_4O_2{}^{79}BrNa$ requires 453.0902 (97.7%) (Diff -1.1 ppm), *m/z* 455.0883 $[M+Na]^+$ $C_{20}H_{23}N_4O_2{}^{81}BrNa$ requires 455.0882 (100%) (Diff 0.3 ppm).

Ethyl ((4-aminobenzyl)carbamoyl)-L-methioninate (14). The crude product was purified by flash column chromatography eluting with 50% EtOAc in hexane to yield a beige foam (305 mg, 0.93 mmol, 81%); ^{1}H NMR (400MHz; CD_3OD; Me_4Si; ppm) δ

7.05 (2H, d, *J* = 8.0), 6.70 (2H, d, *J* = 8.0), 4.45 (1H, dd, *J* = 8.8, 4.8) 4.22-4.17 (4H, m), 2.60-2.51 (2H, m), 2.13-2.04 (4H, m), 1.96-1.86 (1H, m), 1.29 (3H, t, J = 7.2); ^{13}C NMR (100 MHz; CD_3OD; Me_4Si) δ 174.1, 158.0, 144.3, 131.3, 129.1, 114.9, 61.1, 52.2, 44.4, 31.4, 29.7, 15.5, 14.0; HRMS (ES+) *m/z* 326.1531 $[M+H]^+$ $C_{15}H_{24}N_3O_3S$ requires 326.1533. Anal. Calcd. for $C_{15}H_{23}N_3O_3S$: C, 55.36; H, 7.12; N, 12.91; S, 9.85. Found C, 55.10; H, 7.02; N, 12.79; S, 9.67.

Ethyl ((4-aminobenzyl)carbamoyl)-D-methioninate (15). The crude product was purified by flash column chromatography eluting with 50% EtOAc in hexane to yield a beige foam (286 mg, 0.88 mmol, 76%) which was spectroscopically identical to **14**. Anal. Calcd. for $C_{15}H_{23}N_3O_3S$: C, 55.36; H, 7.12; N, 12.91; S, 9.85. Found C, 55.11; H, 7.01; N, 12.92; S, 9.72.

(*S*)-Ethyl 2-(3-(4-(amino)benzyl)ureido)-4-methylpentanoate (16). The crude product was purified by flash column chromatography eluting with 50% EtOAc in hexane to yield a white foam (149 mg, 0.49 mmol, 82%). IR ν_{max} (cm^{-1}) 1183 (C-O), 1516 (N-H), 1555 (N-H), 1631 (amide C=O), 1738 (ester C=O), 2955 (C-H), 3336 (N-H); ^{1}H NMR (400MHz; $CDCl_3$; Me_4Si; ppm) δ 7.07 (2H, d, *J* = 8.3), 6.62 (2H, d, *J* = 8.3), 4.94 (1H, d, *J* = 8.4), 4.84 (1H, t, *J* = 5.3), 4.48 (1H, td, *J* = 8.8, 5.3), 4.22 (2H, 1:1:1:1 q, *J* = 5.2, 2.6), 4.13 (2H, q, *J* = 7.1), 3.65 (2H, br s), 1.66 (1H, q, *J* = 6.6), 1.57 (1H, td, *J* = 8.2, 5.4), 1.45 (1H, td, *J* = 9.1, 5.9), 1.26 (3H, t, *J* = 7.1), 0.93 (6H, t, *J* = 6.6); ^{13}C NMR (100 MHz; $CDCl_3$; Me_4Si) δ 174.7, 157.6, 145.7, 130.1, 128.9, 115.2, 61.2, 51.7, 44.3, 42.1, 24.8, 22.9, 22.0, 14.1; HRMS (ES+) *m/z* 330.1785 $[M+Na]^+$ $C_{16}H_{25}N_3O_3Na$ requires 330.1794. Anal. Calcd. for $C_{16}H_{25}N_3O_3$: C, 62.52; H, 8.20; N, 13.67. Found C, 62.41; H, 8.14; N, 13.70.

(*S*)-1-(4-Aminobenzyl)-3-(4-(methylthio)-1-oxo-1-(pyrrolidin-1-yl)butan-2-yl)urea (17). The crude product was purified by flash column chromatography eluting with

25% EtOAc in hexane to yield a yellow foam (171 mg, 0.49 mmol, 67%); ^{1}H NMR (400MHz; $CDCl_3$; Me_4Si; ppm) δ 7.08 (2H, d, *J* = 7.8), 6.67 (2H, d, *J* = 7.8), 5.86 (2H, br s), 5.11 (1H, br s), 4.89 (1H, br t, *J* = 5.1 Hz), 4.41 (1H, dd, *J* = 8.6, 4.8) 4.15 (2H, d, *J* = 5.0 Hz), 3.31-3.20 (4H, m), 2.60-2.51 (2H, m), 2.15-2.05 (2H, m), 1.92 (3H, s), 1.81 (2H, quintet, *J* = 6.9 Hz), 1.67 (2H, quintet, *J* = 6.9Hz); ^{13}C NMR (100 MHz; $CDCl_3$; Me_4Si) δ 173.9, 157.8, 144.2, 131.5, 128.9, 114.9, 52.3, 44.2, 43.1, 31.6, 29.6, 29.0, 15.6; HRMS (ES+) *m/z* 351.1853 $[M+H]^+$ $C_{17}H_{27}N_4O_2S$ requires 351.1849.

1-(4-Aminobenzyl)-3-((*S*)-4-(methylthio)-1-((*R*)-2-(2-(methylthio)phenyl)pyrrolidin-1-yl)-1-oxobutan-2-yl)urea (18). The reaction yielded a yellow foam as a mixture of 2 rotamers in approximately a 2:1 ratio that required no further purification (18 mg, 0.038 mmol, 72%). IR v_{max} (cm^{-1}) 593 (C-S), 750 (C-H), 1434 (C=C), 1516 (N-H), 1546 (N-H), 1609 (amide C=O), 2918 (C-H), 3340 (N-H); ^{1}H NMR (400MHz; $CDCl_3$; Me_4Si; ppm) δ 7.25 (1H, d, *J* = 2.8, major rotamer), 7.24 (1H, d, *J* = 1.2, minor rotamer), 7.12 (2H, dd, *J* = 5.6, 3.0, minor rotamer), 7.09 (2H, dd, *J* = 5.5, 1.8, major rotamer), 7.03 (2H, d, *J* = 8.3), 7.00 (1H, d, *J* = 3.0, minor rotamer), 6.98 (1H, d, *J* = 3.5, major rotamer), 6.93 (1H, s, major rotamer), 6.91 (1H, s, minor rotamer), 6.62 (3H, dd, *J* = 8.4, 2.1, major rotamer), 6.59 (3H, dd, *J* = 8.4, 2.1, minor rotamer), 6.23 (1H, d, *J* = 9.3, major rotamer), 6.19 (1H, d, *J* = 9.4, minor rotamer), 5.81 (1H, d, *J* = 8.4), 5.58 (1H, t, *J* = 5.2), 5.41 (1H, d, *J* = 8.5, major rotamer), 5.36 (1H, t, *J* = 5.2, minor rotamer), 4.90 (1H, q, *J* = 8.5), 4.36 (1H, td, *J* = 9.6, 3.3), 4.16 (2H, 1:1:1:1 q, *J* = 11.7, 5.3), 3.73 (1H, t, *J* = 8.3, minor rotamer), 3.70 (1H, d, *J* = 9.5, major rotamer), 3.38 (2H, septet, *J* = 15.1, 8.1, 2.9, major rotamer), 3.08 (2H, dt, *J* = 16.2, 8.1, minor rotamer), 2.59 (1H, t, *J* = 7.3), 2.52 (3H, s), 2.35 (3H, s, minor rotamer), 2.11 (3H, s, major rotamer), 1.94 – 1.80 (4H, m);

^{13}C NMR (100 MHz; $CDCl_3$; Me_4Si) δ 171.2, 158.2, 158.2, 145.4, 145.3, 140.8, 139.8, 136.0, 134.9, 129.3, 129.0, 128.6, 128.1, 127.3, 126.3, 126.0, 125.7, 125.2, 124.8, 124.6, 115.2, 115.1, 59.1, 58.9, 50.8, 50.6, 47.9, 47.1, 44.0, 43.7, 33.7, 32.9, 32.5, 32.3, 30.5, 30.2, 23.2, 21.5, 21.1, 16.2, 15.9, 15.7, 15.2; HRMS (ES+) *m/z* 495.1871 $[M+Na]^+$ $C_{24}H_{32}N_4O_2S_2Na$ requires 495.1864 (Diff 1.3 ppm).

1-(4-Aminobenzyl)-3-((*S*)-4-(methylthio)-1-((*S*)-2-(2-(methylthio)phenyl)pyrrolidin-1-yl)-1-oxobutan-2-yl)urea (19). The reaction yielded a yellow foam as a mixture of 2 rotamers in approximately a 2:1 ratio that required no further purification (31 mg, 0.066 mmol, 84%). IR v_{max} (cm^{-1}) 602 (C-S), 748 (C-H), 1432 (C=C), 1515 (N-H), 1548 (N-H), 1612 (amide C=O), 2918 (C-H), 3337 (N-H); ^{1}H NMR (400MHz; $CDCl_3$; Me_4Si; ppm) δ 7.23 (1H, d, *J* = 5.8), 7.15 (2H, t, *J* = 8.4, major rotamer), 7.06 (2H, t, *J* = 7.4, minor rotamer), 6.98 (2H, d, *J* = 8.3, major rotamer), 6.86 (2H, d, *J* = 7.4, minor rotamer), 6.58 (2H, d, *J* = 8.3), 6.23 (1H, d, *J* = 8.4, major rotamer), 5.86 (1H, d, *J* = 7.6, minor rotamer), 5.58 (1H, t, *J* = 5.8), 5.34 (1H, dd, *J* = 7.6, 2.6), 4.91 (1H, q, *J* = 7.9), 4.20 (1H, d, *J* = 5.5), 3.97 (1H, dd, *J* = 17.8, 8.2), 3.89 (1H, dd, *J* = 11.3, 5.7), 3.23 (3H, q, *J* = 8.6), 2.49 – 2.43 (2H, m), 2.36 (3H, s), 2.21 – 2.11 (1H, m), 2.07 (3H, s, major rotamer), 2.03 (3H, s, minor rotamer), 1.93 (3H, septet, *J* = 25.4, 13.6, 5.9), 1.83 (1H, q, *J* = 7.9), 1.74 (2H, q, *J* = 8.0); ^{13}C NMR (100 MHz; $CDCl_3$; Me_4Si) δ 172.0, 171.2, 158.1, 157.1, 145.0, 140.4, 139.6, 135.5, 135.2, 129.9, 128.7, 128.6, 128.5, 128.2, 127.5, 126.6, 126.1, 125.4, 124.9, 123.9, 115.3, 115.1, 58.6, 58.5, 51.2, 50.4, 48.2, 47.3, 43.7, 43.5, 34.0 34.1, 33.0, 32.1, 30.2, 30.1, 21.2, 21.1, 16.4, 15.8, 15.6, 15.5; HRMS (ES+) *m/z* 495.1862 $[M+Na]^+$ $C_{24}H_{32}N_4O_2S_2Na$ requires 495.1864 (Diff -0.5 ppm).

Supporting Information More details on molecular docking, crystallisation and cellular assays are provided. This material is available free of charge via the Internet at http://pubs.acs.org.

PDB Codes: 5CBT, 5CBU, 5CBV, 5CCN, 5CBW, 5CCS, 5CCR

AUTHOR INFORMATION

Corresponding Authors

Phone: +44 151 794 3553 E-mail: pmoneill@liverpool.ac.uk

Phone: +44 151 795 4458 E-mail: lu-yun.lian@liverpool.ac.uk.

Author Contributions

E R Shore and M Awais contributed equally.

ABBREVIATIONS USED

$\Delta\Psi_m$, mitochondrial membrane potential; ΔH, change in enthalpy; ΔS, change in entropy; CsA, cyclosporine; Cyp, Cyclophilin; ITC, Isothermal titration calorimetry; MPTP, Mitochondrial permeability transition pore; PAC, pancreatic acinar cells; PPIase, peptidyl-prolyl isomerase;RMSD, Root mean square deviation; TLCS, taurolithocholate acid 3-sulphate; TMRM, tetramethyl rhodamine methyl ester.

ACKNOWLEDGEMENTS

This work was supported by the UK NIHR Biomedical Research Unit Funding Scheme and the Engineering and Physical Sciences Research Council (DTA Studentship to ERS (EP/K503095/1)). We thank the staff and management of SOLEIL for provision of the crystallographic facilities at their synchrotron centres. Use of SOLEIL was funded by the European Community's Seventh Framework Program (FP7/2007-2013) under BioStruct-X Grant 283570 and Proposals 2370/5437. We thank M. McCarron and J. Ellis, Department of Chemistry, University of Liverpool for performing the mass spectrometry and elemental microanalyses.

REFERENCES

1. Pandol, S. J.; Saluja, A. K.; Imrie, C. W.; Banks, P. A. Acute pancreatitis: bench to the bedside. *Gastroenterology* **2007,** 132, 1127-51.

2. Petrov, M. S.; Shanbhag, S.; Chakraborty, M.; Phillips, A. R.; Windsor, J. A. Organ failure and infection of pancreatic necrosis as determinants of mortality in patients with acute pancreatitis. *Gastroenterology* **2010,** 139, 813-20.

3. Wu, B. U.; Banks, P. A. Clinical management of patients with acute pancreatitis. *Gastroenterology* **2013,** 144, 1272-81.

4. Mukherjee, R.; Mareninova, O. A.; Odinokova, I. V.; Huang, W.; Murphy, J.; Chvanov, M.; Javed, M. A.; Wen, L.; Booth, D. M.; Cane, M. C.; Awais, M.; Gavillet, B.; Pruss, R. M.; Schaller, S.; Molkentin, J. D.; Tepikin, A. V.; Petersen, O. H.; Pandol, S. J.; Gukovsky, I.; Criddle, D. N.; Gukovskaya, A. S.; Sutton, R.; and, N. P. B. R. U. Mechanism of mitochondrial permeability transition pore induction and damage in the pancreas: inhibition prevents acute pancreatitis by protecting production of ATP. *Gut* **2015**.

5. Lerch, M. M.; Halangk, W.; Mayerle, J. Preventing pancreatitis by protecting the mitochondrial permeability transition pore. *Gastroenterology* **2013,** 144, 265-9.

6. Halestrap, A. P.; Richardson, A. P. The mitochondrial permeability transition: a current perspective on its identity and role in ischaemia/reperfusion injury. *J. Mol. Cell. Cardiol.* **2015,** 78, 129-41.

7. Malty, R. H.; Jessulat, M.; Jin, K.; Musso, G.; Vlasblom, J.; Phanse, S.; Zhang, Z.; Babu, M. Mitochondrial targets for pharmacological intervention in human disease. *Journal of proteome research* **2015,** 14, 5-21.

8. Celsi, F.; Pizzo, P.; Brini, M.; Leo, S.; Fotino, C.; Pinton, P.; Rizzuto, R. Mitochondria, calcium and cell death: a deadly triad in neurodegeneration. *Biochim. Biophys. Acta* **2009,** 1787, 335-44.

9. Cruthirds, D. L.; Novak, L.; Akhi, K. M.; Sanders, P. W.; Thompson, J. A.; MacMillan-Crow, L. A. Mitochondrial targets of oxidative stress during renal ischemia/reperfusion. *Arch. Biochem. Biophys.* **2003,** 412, 27-33.

10. Millay, D. P.; Sargent, M. A.; Osinska, H.; Baines, C. P.; Barton, E. R.; Vuagniaux, G.; Sweeney, H. L.; Robbins, J.; Molkentin, J. D. Genetic and pharmacologic inhibition of mitochondrial-dependent necrosis attenuates muscular dystrophy. *Nat. Med.* **2008,** 14, 442-7.

11. Nakagawa, T.; Shimizu, S.; Watanabe, T.; Yamaguchi, O.; Otsu, K.; Yamagata, H.; Inohara, H.; Kubo, T.; Tsujimoto, Y. Cyclophilin D-dependent mitochondrial permeability transition regulates some necrotic but not apoptotic cell death. *Nature* **2005,** 434, 652-8.

12. Baines, C. P.; Kaiser, R. A.; Purcell, N. H.; Blair, N. S.; Osinska, H.; Hambleton, M. A.; Brunskill, E. W.; Sayen, M. R.; Gottlieb, R. A.; Dorn, G. W.; Robbins, J.; Molkentin, J. D. Loss of cyclophilin D reveals a critical role for mitochondrial permeability transition in cell death. *Nature* **2005,** 434, 658-62.

13. Fischer, G.; Bang, H.; Mech, C. [Determination of enzymatic catalysis for the cis-trans-isomerization of peptide binding in proline-containing peptides]. *Biomed Biochim Acta* **1984,** 43, 1101-11.

14. Fischer, G.; Schmid, F. X. The mechanism of protein folding. Implications of in vitro refolding models for de novo protein folding and translocation in the cell. *Biochemistry* **1990,** 29, 2205-2212.

15. Fischer, G.; Wittmann-Liebold, B.; Lang, K.; Kiefhaber, T.; Schmid, F. X. Cyclophilin and peptidyl-prolyl cis-trans isomerase are probably identical proteins. *Nature* **1989,** 337, 476-478.

16. Elrod, J. W.; Molkentin, J. D. Physiologic functions of cyclophilin D and the mitochondrial permeability transition pore. *Circ. J.* **2013,** 77, 1111-22.

17. Giorgio, V.; von Stockum, S.; Antoniel, M.; Fabbro, A.; Fogolari, F.; Forte, M.; Glick, G. D.; Petronilli, V.; Zoratti, M.; Szabo, I.; Lippe, G.; Bernardi, P. Dimers of mitochondrial ATP synthase form the permeability transition pore. *Proc. Natl. Acad. Sci. U. S. A.* **2013,** 110, 5887-92.

18. Alavian, K. N.; Beutner, G.; Lazrove, E.; Sacchetti, S.; Park, H. A.; Licznerski, P.; Li, H.; Nabili, P.; Hockensmith, K.; Graham, M.; Porter, G. A., Jr.; Jonas, E. A. An uncoupling channel within the c-subunit ring of the F1FO ATP synthase is the mitochondrial permeability transition pore. *Proc. Natl. Acad. Sci. U. S. A.* **2014,** 111, 10580-5.

19. Gaither, L. A.; Borawski, J.; Anderson, L. J.; Balabanis, K. A.; Devay, P.; Joberty, G.; Rau, C.; Schirle, M.; Bouwmeester, T.; Mickanin, C.; Zhao, S.; Vickers, C.; Lee, L.; Deng, G.; Baryza, J.; Fujimoto, R. A.; Lin, K.; Compton, T.; Wiedmann, B. Multiple cyclophilins involved in different cellular pathways mediate HCV replication. *Virology* **2010,** 397, 43-55.

20. Hopkins, S.; Gallay, P. Cyclophilin inhibitors: an emerging class of therapeutics for the treatment of chronic hepatitis C infection. *Viruses* **2012,** 4, 2558-77.

21. Liu, J.; Farmer, J. D., Jr.; Lane, W. S.; Friedman, J.; Weissman, I.; Schreiber, S. L. Calcineurin is a common target of cyclophilin-cyclosporin A and FKBP-FK506 complexes. *Cell* **1991,** 66, 807-15.

22. Dunsmore, C. J.; Malone, K. J.; Bailey, K. R.; Wear, M. A.; Florance, H.; Shirran, S.; Barran, P. E.; Page, A. P.; Walkinshaw, M. D.; Turner, N. J. Design and synthesis of conformationally constrained cyclophilin inhibitors showing a cyclosporin-A phenotype in C. elegans. *Chembiochem : a European journal of chemical biology* **2011,** 12, 802-10.

23. Ni, S.; Yuan, Y.; Huang, J.; Mao, X.; Lv, M.; Zhu, J.; Shen, X.; Pei, J.; Lai, L.; Jiang, H.; Li, J. Discovering potent small molecule inhibitors of cyclophilin A using de novo drug design approach. *J. Med. Chem.* **2009,** 52, 5295-8.

24. Guichou, J. F.; Colliandre, L.; Ahmed-Belkacem, H.; Pawlotsky, J. M. New Inhibitors of Cyclophilins and uses thereof. *Patent WO2011/076784* **2010**.

25. Guichou, J. F.; Colliandre, L.; Ahmed-Belkacem, H.; Pawlotsky, J. M. New Inhibitors of Cyclophilins and uses thereof. *Patent US2013/0018044* **2013**.

26. Guichou, J. F.; Viaud, J.; Mettling, C.; Subra, G.; Lin, Y. L.; Chavanieu, A. Structure-based design, synthesis, and biological evaluation of novel inhibitors of human cyclophilin A. *J. Med. Chem.* **2006,** 49, 900-10.

27. Feng, B. Y.; Shoichet, B. K. A detergent-based assay for the detection of promiscuous inhibitors. *Nat. Protocols* **2006,** 1, 550-553.

28. Ryan, A. J.; Gray, N. M.; Lowe, P. N.; Chung, C.-w. Effect of Detergent on "Promiscuous" Inhibitors. *J. Med. Chem.* **2003,** 46, 3448-3451.

29. Kalgutkar, A. S.; Gardner, I.; Obach, R. S.; Shaffer, C. L.; Callegari, E.; Henne, K. R.; Mutlib, A. E.; Dalvie, D. K.; Lee, J. S.; Nakai, Y.; O'Donnell, J. P.; Boer, J.; Harriman, S. P. A comprehensive listing of bioactivation pathways of organic functional groups. *Curr. Drug Metab.* **2005,** 6, 161-225.

30. Nassar, A. E.; Kamel, A. M.; Clarimont, C. Improving the decision-making process in the structural modification of drug candidates: enhancing metabolic stability. *Drug Discov. Today* **2004,** 9, 1020-8.

31. Cui, Z.; Yu, H.-J.; Yang, R.-F.; Gao, W.-Y.; Feng, C.-G.; Lin, G.-Q. Highly Enantioselective Arylation of N-Tosylalkylaldimines Catalyzed by Rhodium-Diene Complexes. *J. Am. Chem. Soc.* **2011,** 133, 12394-12397.

32. Hou, G.-H.; Xie, J.-H.; Yan, P.-C.; Zhou, Q.-L. Iridium-Catalyzed Asymmetric Hydrogenation of Cyclic Enamines. *J. Am. Chem. Soc.* **2009,** 131, 1366-1367.

33. Klebe, G. Applying thermodynamic profiling in lead finding and optimization. *Nat. Rev. Drug. Discov.* **2015,** 14, 95-110.

34. Kajitani, K.; Fujihashi, M.; Kobayashi, Y.; Shimizu, S.; Tsujimoto, Y.; Miki, K. Crystal structure of human cyclophilin D in complex with its inhibitor, cyclosporin A at 0.96-Å resolution. *Proteins* **2008,** 70, 1635-1639.

35. Singh, R. K.; Suzuki, T.; Mandal, T.; Balsubramanian, N.; Haldar, M.; Mueller, D. J.; Strode, J. A.; Cook, G.; Mallik, S.; Srivastava, D. K. Thermodynamics of Binding of Structurally Similar Ligands to Histone Deacetylase 8 Sheds Light on Challenges in the Rational Design of Potent and Isozyme-Selective Inhibitors of the Enzyme. *Biochemistry* **2014,** 53, 7445-7458.

36. Eisenmesser, E. Z.; Millet, O.; Labeikovsky, W.; Korzhnev, D. M.; Wolf-Watz, M.; Bosco, D. A.; Skalicky, J. J.; Kay, L. E.; Kern, D. Intrinsic dynamics of an enzyme underlies catalysis. *Nature* **2005,** 438, 117-121.

37. Ramanathan, A.; Savol, A.; Burger, V.; Chennubhotla, C. S.; Agarwal, P. K. Protein conformational populations and functionally relevant substates. *Acc. Chem. Res.* **2014,** 47, 149-56.

38. Davis, T. L.; Walker, J. R.; Campagna-Slater, V.; Finerty, P. J.; Paramanathan, R.; Bernstein, G.; MacKenzie, F.; Tempel, W.; Ouyang, H.; Lee, W. H.; Eisenmesser, E. Z.; Dhe-Paganon, S. Structural and biochemical characterization of the human cyclophilin family of peptidyl-prolyl isomerases. *PLoS Biol.* **2010,** 8, e1000439.

39. Petersen, O. H.; Tepikin, A. V. Polarized calcium signaling in exocrine gland cells. *Annu. Rev. Physiol.* **2008,** 70, 273-99.

40. Gerasimenko, J. V.; Flowerdew, S. E.; Voronina, S. G.; Sukhomlin, T. K.; Tepikin, A. V.; Petersen, O. H.; Gerasimenko, O. V. Bile acids induce Ca2+ release from both the endoplasmic reticulum and acidic intracellular calcium stores through activation of inositol trisphosphate receptors and ryanodine receptors. *J. Biol. Chem.* **2006,** 281, 40154-63.

41. Wen, L.; Voronina, S.; Javed, M. A.; Awais, M.; Szatmary, P.; Latawiec, D.; Chvanov, M.; Collier, D.; Huang, W.; Barrett, J.; Begg, M.; Stauderman, K.; Roos, J.; Grigoryev, S.; Ramos, S.; Rogers, E.; Whitten, J.; Velicelebi, G.; Dunn, M.; Tepikin, A. V.; Criddle, D. N.; Sutton, R. Inhibitors of ORAI1 Prevent Cytosolic Calcium-Associated Injury of Human Pancreatic Acinar Cells and Acute Pancreatitis in 3 Mouse Models. *Gastroenterology* **2015,** 149, 481-492 e7.

42. Booth, D. M.; Murphy, J. A.; Mukherjee, R.; Awais, M.; Neoptolemos, J. P.; Gerasimenko, O. V.; Tepikin, A. V.; Petersen, O. H.; Sutton, R.; Criddle, D. N. Reactive oxygen species induced by bile acid induce apoptosis and protect against necrosis in pancreatic acinar cells. *Gastroenterology* **2011,** 140, 2116-25.

Table 1: Summary of Chemical Structures, Thermodynamic Parameters, Binding and Inhibition Constants, and Crystal Structures Accession Codes.

Compound	Ar	R	X	ΔG (kcal/mol)	ΔH (kcal/mol)	TΔS (kcal/mol)	K_d (μM)[¥]	K_i (μM)[#]	Crystal Structure
CsA	-	-	-	-10.74	-14.7	-3.96	0.013	0.0082	2Z6W
4$^+$		H	OEt	-6.82	-13.70	-6.88	10.0	5.9	3RDC
5$^+$		H	OEt	-5.47	-1.98	3.49	97.3	63	5CBT[$]
6	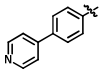	H	OEt	-5.47	-1.24	4.23	97.3	ND[¨]	5CBU[$]
7		H	OEt	-5.31	-2.33	2.98	127	ND[¨]	5CBV[$]
8		H	OEt	-5.50	-1.77	3.73	92.5	22	5CCN[$]
9		H	OEt	-6.09	-0.73	5.36	34.1	2.6	5CBW[$]
10$^+$		H		-6.34	-4.99	1.35	22.7	4.9	4J58
11		H		-7.19	-9.51	-2.32	5.4	ND[¨]	5CCS [$]
12$^+$		H		-7.57	-10.32	2.75	2.8	ND[¨]	4J5B
13$^+$		H		-8.05	-4.56	3.49	1.2	0.95	4J5D
14$^+$			OEt	-7.20	-13.54	-6.31	5.12	9.1	5CCR[$]
15$^+$			OEt	-[&]	-[&]	-[&]	-[&]	ND[¨]	ND[¨]
16$^+$			OEt	-6.89	-14.82	-7.93	8.8	ND[¨]	ND[¨]
17				-5.78	-6.63	-0.85	57.6	ND[¨]	ND[¨]
18$^+$				-5.60	-1.1	5.48	82	ND[¨]	4J5C
19$^+$				-8.71	-12.49	-3.78	0.41	0.099	4J5C

[¥]K_d values recorded by ITC in μM at 25°C, [#] K_i values recorded by PPIase assay at fixed substrate concentration but varying inhibitor concentrations at 10°C, [+]Compounds reported in the patents published by Colliandre *et al.* ¨ND: not determined, [$] New crystal structures from this work, [&] Extremely weak binding.

FIGURE LEGENDS

Figure 1. Structures of Cyclosporin A, Debio 025 and NIM811.

Figure 2. Structures of reported Cyp inhibitors.

Figure 3. Definition of binding sites. (a) Crystal structure of compound **4** in complex with CypD (PDB: 3RDC) with S1' and S2 defined as the prolyl and residue -2, -3 binding sites respectively. (b, c and d) Schematic with definition of the sites of peptide, CsA and compound **4** binding, respectively.

Figure 4. ITC profiles for the binding of selected compounds to CypD. (a) Compound **4** (b) Compound **10** (c) Compound **12** (d) Compound **14** (e) Compound **11** and (f) Compound **19**. The top panel shows the raw calorimetric data obtained upon titration of CypD with each ligand; the bottom panel shows the plots of the integrated heat signal as a function of molar ratio of ligand to protein. The data fit to a one-site binding to yield the K_d, ΔH and ΔS parameters (Table 1).

Figure 5. Thermodynamic signatures for the binding of the different compounds listed in Table 1. (a) Compounds **4-9**, Cyclosporin A (CsA). Note the marked difference in the ΔH and ΔS between **4** and **5-9** although ΔG (and hence Kd) are similar, showing an enthalpy-entropy compensation effect. (b, c) Compounds **10-19** show the progressive improvement.

Figure 6. Crystal structure data for CypD complexes. (a, b) Surface representation of CypD in complex with compounds **4** (PDB: 3RDC) (a) and **6** (PDB: 5CBU) (b) highlighting the S2 and S1' ligand binding pockets. Note the difference in the size of the S2 pocket between the two structures. (c) Orientations of Arg82 side chain in the structures of complexes with compounds **4** and **6**. (d) Overlay of complexes with **4** and **11** (PDB: 5CCS) showing an expanded view of the S1' binding site with stick representations of **4** (yellow) and **11** (pink). Note the difference in the orientations of

Arg55 side-chains in the two structures. Representative hydrogen bonds between Arg55 and **4** and **11** are shown in, respectively, black and yellow dash lines. In all the figures, the compounds numbers are in square boxes. (e) Amino acid sequence of mature recombinant CypD. Figure produced using The PyMOL Molecular Graphics System, Version 1.3.1 Schrödinger, LLC.

Figure 7. Crystal structure of **19** bound to CypD. **19** is rendered as sticks (carbon – cyan, nitrogen – blue, oxygen – red, sulphur - yellow). Residues involved in non-covalent interactions are rendered as thin sticks (carbon – green, nitrogen – blue, oxygen – red). Crystallised waters rendered as red spheres. Non-covalent contacts are shown as dotted lines with the colour code given in the key. Non-covalent contacts analysed with ViewContacts software (*J. Chem. Inf. Model.*, 2011, **51**, 3180-3198). Figure rendered in PyMOL Molecular Graphics System, Version 1.3.1 Schrödinger, LLC. The amino acid numbering is as shown in Figure 6.

Figure 8. Effect of small molecule inhibitors on freshly isolated PACs in the presence of TLCS. (a) Inhibition of necrotic cell death pathway activation by inhibitors CsA, **4**, **13**, **14**, or **19** in murine PACs induced by TLCS (500 μM) (mean ± s.e.m., normalised to TLCS; n = 3 experiments/group; *$p<0.05$, TLCS vs inhibitor + TLCS groups). Propidium iodine (PI) uptake by cells represents necrotic cell death. (b) Protection of $\Delta\psi_m$ of murine PACs by inhibitors **13**, **14** or **19** at 10 μM in the presence of TLCS (500 μM). TMRM fluorescence is shown as normalised (F/F_0) mean ± SEM; F_0 is an average fluorescence of TMRM baseline. (c) Inhibition of necrotic cell death pathway activation induced by TLCS (500 μM) by **19** at 10 μM in human PACs. The graph is based on one experiment/group using isolated human PACs [3 wells and 12 high-power fields each; total: 166 control cells, 223 TLCS and 179 inhibitor **19** plus TLCS], *$p<0.05$, TLCS vs **19** plus TLCS

Figures, Schemes

Scheme 1[a]

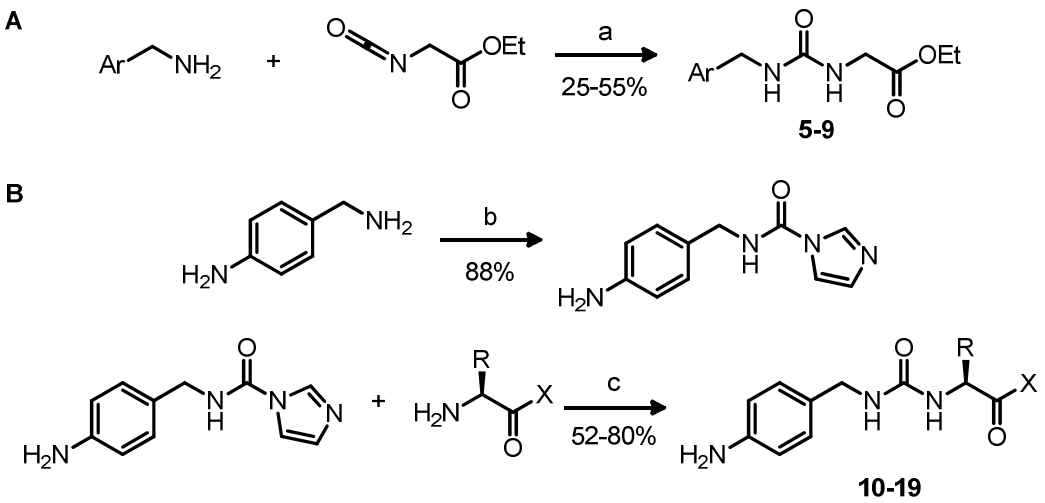

[a]Reagents and conditions: a) DMF, rt, 2 h; b) CDI, DMAP, DCM; c) NEt_3, DMAP, CH_3CN, rt, 24 h.

Scheme 2[a]

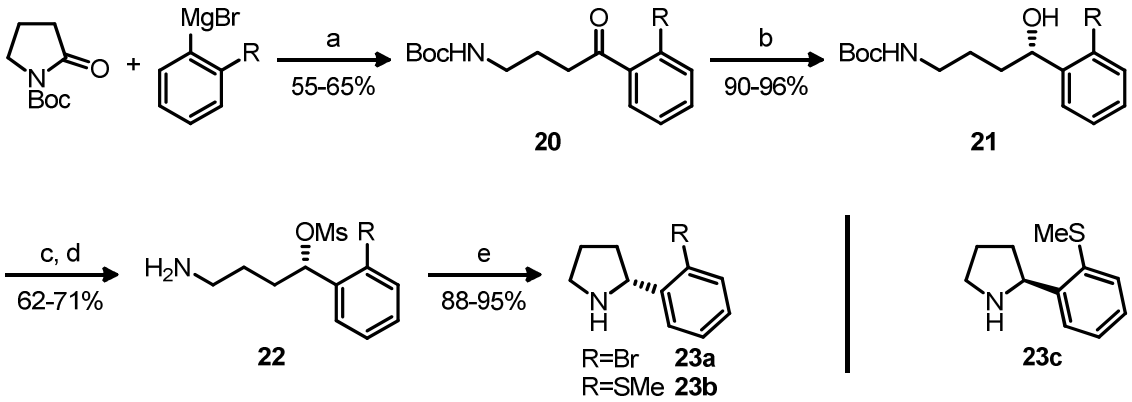

[a]Reagents and conditions: a) THF, −78 °C to rt, 16 h; b) (*R*)-CBS, BH_3.DMS, rt, 24 h; c) MsCl, Et_3N, CH_2Cl_2, 0 °C to rt, 16 h; d) TFA, CH_2Cl_2, rt, 2 h; e) NaOH, MeOH, rt, 16 h.

Figure 1

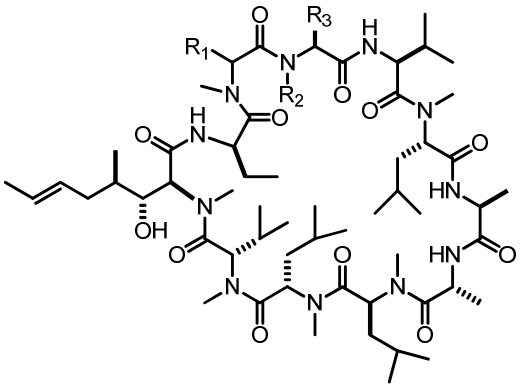

	R_1	R_2	R_3
CsA	**H**	**Me**	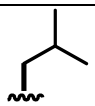
Debio025	**Me**	**Et**	
NIM811	**H**	**Et**	

Figure 2

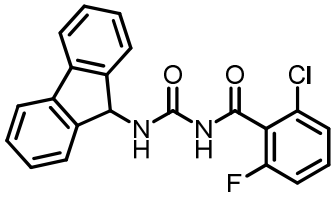

1

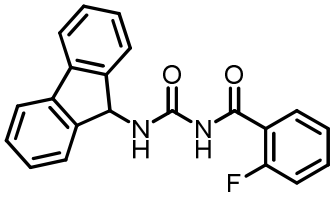

2

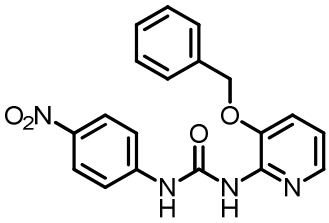

3

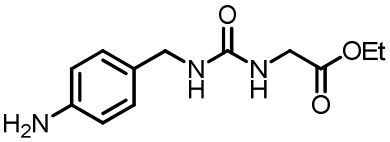

4

Figure 3

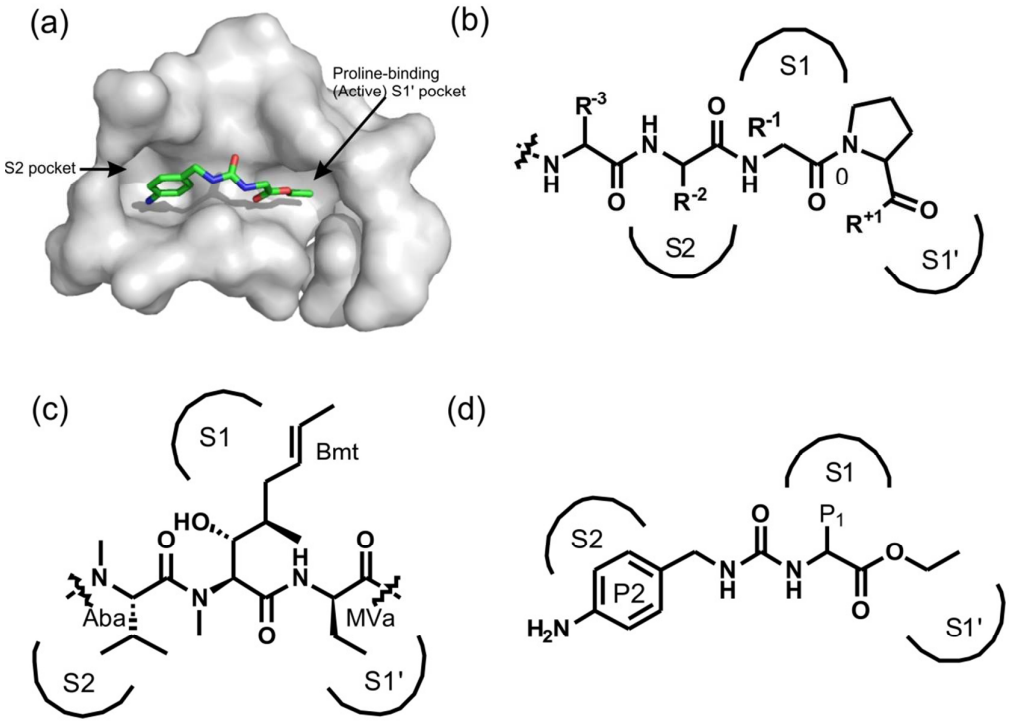
(a)
Proline-binding
(Active) S1' pocket
S2 pocket
(b)
S1
S2
S1'
(c)
S1
Bmt
HO
Aba
MVa
S2
S1'
(d)
S1
S2
P2
S1'

Figure 4

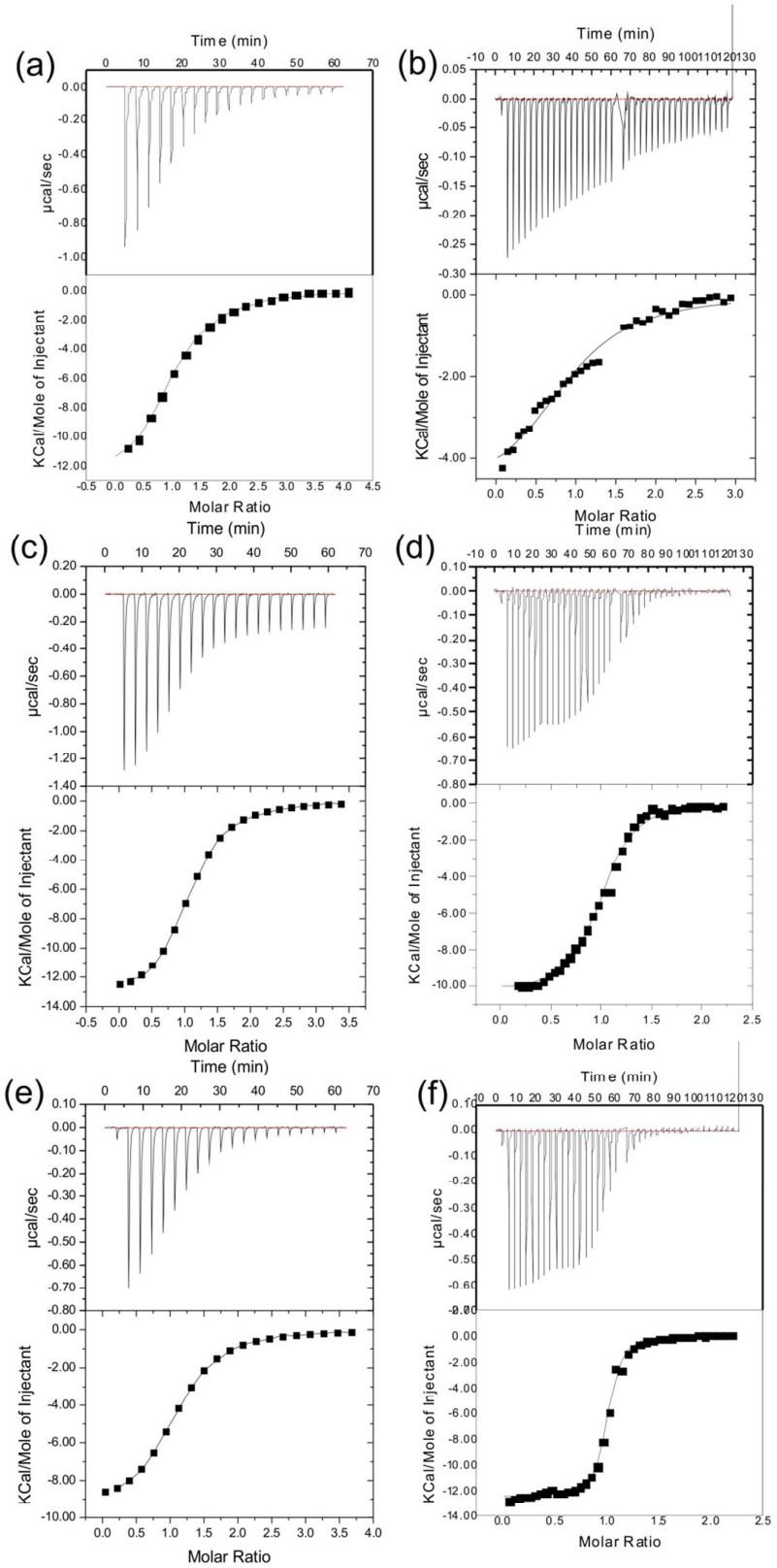

Figure 5

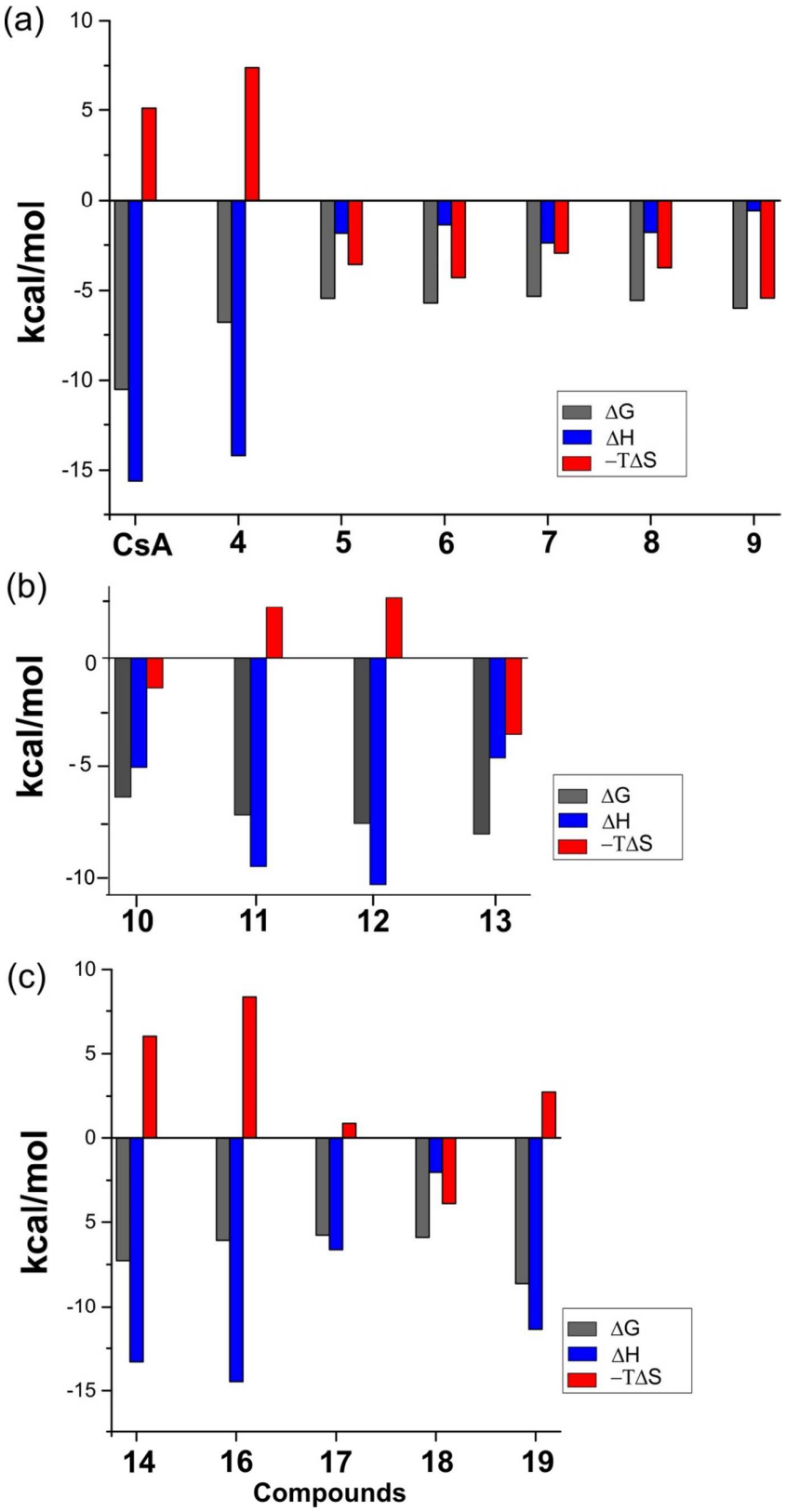
(a)
kcal/mol
10
5
0
-5
-10
-15
ΔG
ΔH
−TΔS
CsA
4
5
6
7
8
9
(b)
kcal/mol
0
-5
-10
ΔG
ΔH
−TΔS
10
11
12
13
(c)
kcal/mol
10
5
0
5
-10
-15
ΔG
ΔH
−TΔS
14
16
17
18
19
Compounds

Figure 6

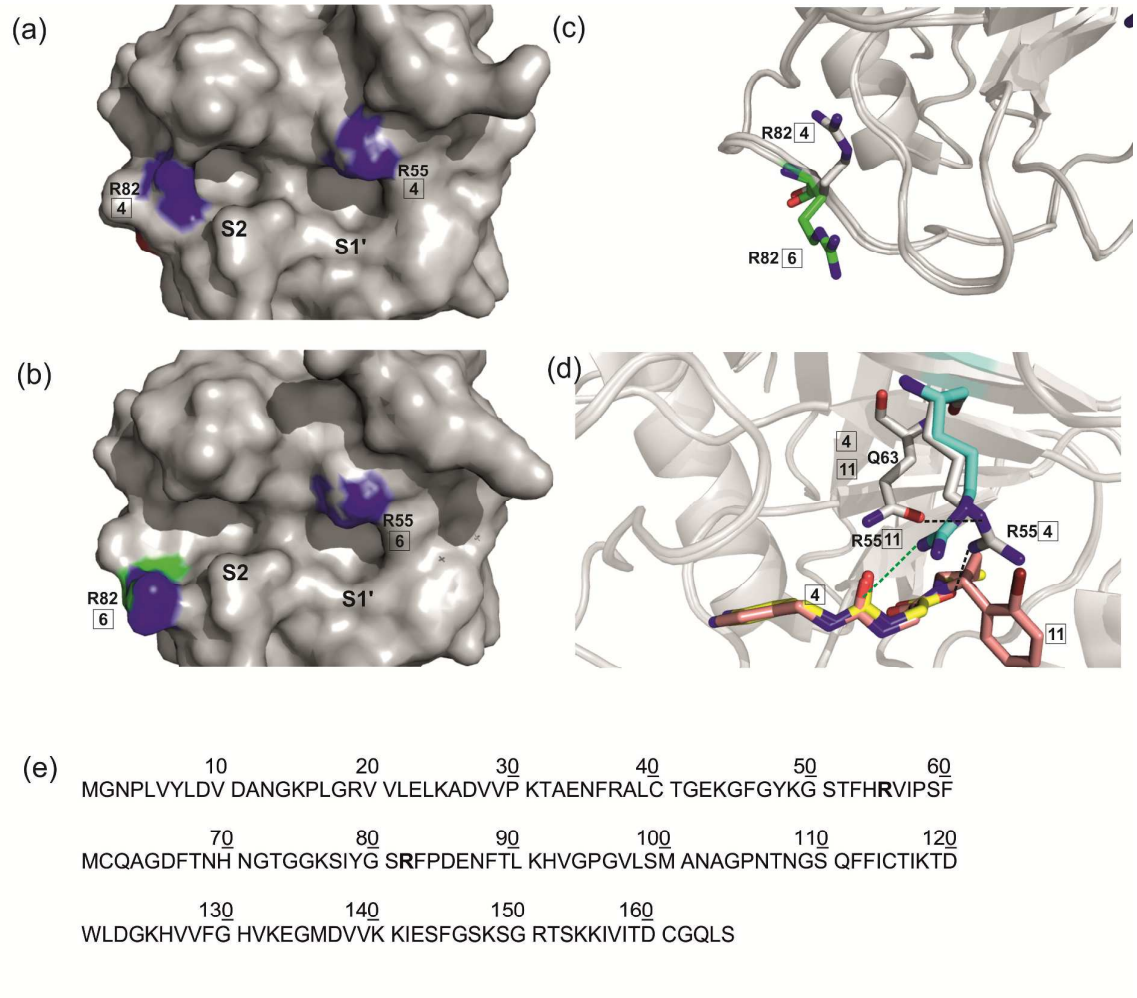
(a)
R82
4
R55
4
S2
S1'
(b)
R55
6
S2
R82
6
S1'
(c)
R82 4
R82 6
(d)
4
11
Q63
R55 11
R55 4
4
11
(e)
10 20 30 40 50 60
MGNPLVYLDV DANGKPLGRV VLELKADVVP KTAENFRALC TGEKGFGYKG STFHRVIPSF
70 80 90 100 110 120
MCQAGDFTNH NGTGGKSIYG SRFPDENFTL KHVGPGVLSM ANAGPNTNGS QFFICTIKTD
130 140 150 160
WLDGKHVVFG HVKEGMDVVK KIESFGSKSG RTSKKIVITD CGQLS

Figure 7

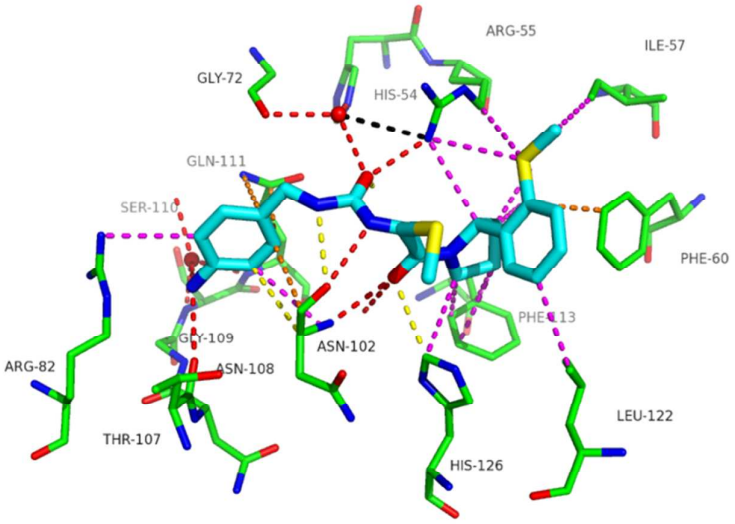

	Non-covalent interaction
▪▪▪▪▪	Hydrogen bond
▪▪▪▪▪	Cation-dipole
▪▪▪▪▪	Hydrogen bond-π
▪▪▪▪▪	π- π
▪▪▪▪▪	Van der Waals

Figure 8a

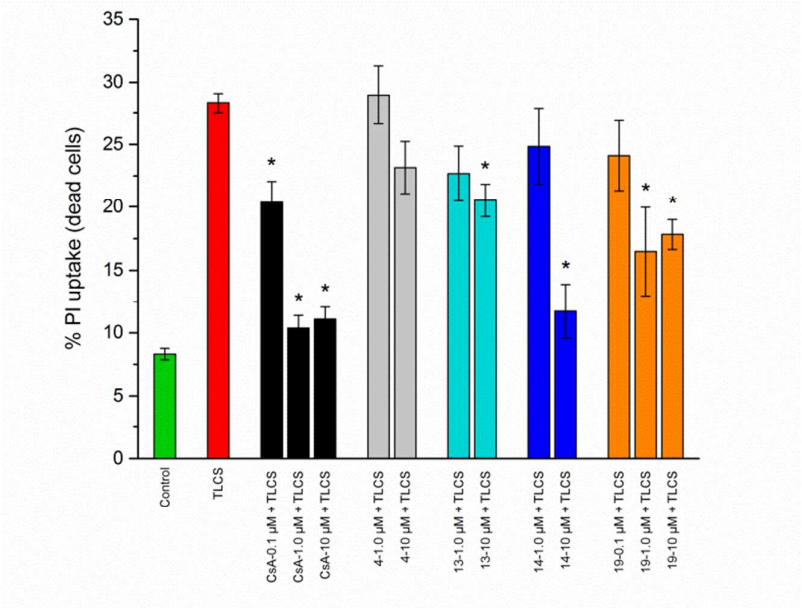

8b

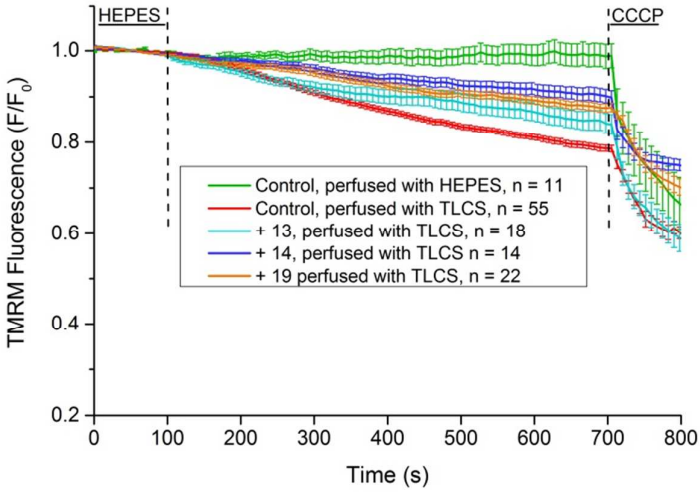

8c

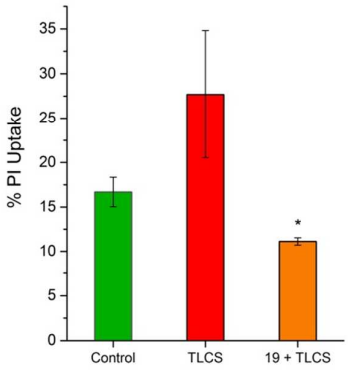
% PI Uptake
35
30
25
20
15
10
5
0
*
Control
TLCS
19 + TLCS

1

TOC Figure